IDŐJÁRÁS

QUARTERLY JOURNAL
OF THE HUNGARIAN METEOROLOGICAL SERVICE

CONTENTS

****

http://omsz.met.hu/english/ref/jurido/jurido_en.html

VOL. 109 * NO. 1 * JANUARY - MARCH 2005

IDŐJÁRÁS

Quarterly Journal of the Hungarian Meteorological Service

Editorial Office: P.O. Box 39, H-1675 Budapest, Hungary or
Gilice tér 39, H-1181 Budapest, Hungary
E-mail: bozo.l@met.hu or *antal.e@met.hu*
Fax: (36-1) 346-4809

Subscription by

mail: IDŐJÁRÁS, P.O. Box 39, H-1675 Budapest, Hungary;
E-mail: bozo.l@met.hu or *antal.e@met.hu*; *Fax: (36-1) 346-4809*

IDŐJÁRÁS

Quarterly Journal of the Hungarian Meteorological Service
Vol. 109, No. 1, January–March 2005, pp. 1–20

Tendencies of extreme climate indices based on daily precipitation in the Carpathian Basin for the 20th century

Judit Bartholy and **Rita Pongrácz**

Department of Meteorology, Eötvös Loránd University,
P.O. Box 32, H-1518 Budapest, Hungary
E-mails: bari@ludens.elte.hu; prita@elte.hu

(Manuscript received in final form November 10, 2004)

Abstract—Precipitation is one of the most important elements of the hydrological cycle, and extreme events associated with precipitation are considered a key factor in several types of human activities, including agriculture, for instance. Therefore, the main objective of this paper is to evaluate extreme precipitation indices. Several climate extreme indices have been analyzed and compared for the entire world, the European continent, and the Carpathian Basin for the second half of the twentieth century according to the guidelines suggested by the joint WMO-CCl/CLIVAR Working Group (formed at the end of the 1990s) on climate change detection. These extreme precipitation indices include the number of wet days using several threshold values, e.g., 20 mm (RR20), 10 mm (RR10), 5 mm (RR5), 1 mm (RR1), 0.1 mm (RR0.1), the upper quartile and the 95th percentile of daily precipitation in the baseperiod 1961–1990 (R75 and R95); the maximum number of consecutive dry days (CDD); the highest 1-day precipitation amount (Rx1); the greatest 5-day rainfall total (Rx5); the annual fraction due to extreme precipitation events (R95T); simple daily intensity index (SDII); etc. Our results suggest that regional intensity and frequency of extreme precipitation increased in the Carpathian Basin during the second half of the twentieth century, while the total precipitation decreased, and the mean climate became slightly drier.

Key-words: extremes, climate index, daily precipitation, Carpathian Basin, Europe, tendency analysis

1. Introduction

National meteorological services usually monitor climate means, tendencies, and extremes only for their own region. First, *IPCC* (1995) declared the global warming trend of the last 150 years due to anthropogenic activity, which increased the annual global mean temperature by 0.7 °C. This IPCC report also

concluded that changes in both the mean and extreme climate parameters may strongly affect human and natural systems. In the mean time, several research projects published results on the analysis of climate extremes on global or continental scales (e.g., *Nicholls et al.*, 1996; *Folland et al.*, 2000; *Easterling et al.*, 2000; *Peterson et al.*, 2002). Furthermore, the Workshop on Indices and Indicators for Climate Extremes was held in Asheville, North Carolina, on June 3–6, 1997. The main objectives of this meeting were to determine the required data sets for climate extreme analysis on larger scales, and to compile the list of climate extreme indices suggested for the global analysis (*Karl et al.*, 1999). Then, in 1998, a joint WMO-CCl/CLIVAR Working Group formed on climate change detection; one of its task groups aimed to identify the climate extreme indices and completed a climate extreme analysis on all part of the world where appropriate data was available (*Frich et al.*, 2002). Some results of this working group also appeared in *IPCC* (2001).

The next section of this paper summarizes and compares the results of the global (*Frich et al.*, 2002) and European (*Klein Tank* and *Können*, 2003) extreme precipitation analysis. Similar methodology has been applied to precipitation extremes of the Carpathian Basin. Section 3 discusses the differences between continental (for Europe) and regional (for the Carpathian Basin) extreme tendencies. Section 4 presents detailed analysis of regional extreme precipitation indices for Hungary. Finally, Section 5 concludes the main findings of this paper.

2. Definition of extreme indices based on daily precipitation, comparison of the global and European analyses

In order to compile a global climate database suitable for extreme analysis, the CCl/CLIVAR task group on extreme indices contacted the national meteorological services and collected daily precipitation, maximum, minimum, and mean temperature time series for the period 1946–1999. Beside data from the national meteorological services, sources include the NOAA NCDC datasets (*Peterson* and *Vose*, 1997), the European Climate Assessment Dataset (*Klein Tank et al.*, 2002b), and daily meteorological time series for Australia (*Trewin*, 1999). All these datasets have been quality controlled and adjusted for inhomogeneities. Then, in order to include a given observation station, the following general criteria have been used: (i) from the entire 1946–1999 period data must be available for at least 40 years; (ii) missing data cannot be more than 10%; (iii) missing data from each year cannot exceed 20%; (iv) more than 3 months consecutive missing values are not allowed each year. In spite

of all these selection criteria, results of any analysis are strongly dependent on the precipitation series themselves, including the instrumental issues.

The CCl/CLIVAR task group decided to map station data instead of gridded database, since extreme events (e.g., local floods and droughts, heat waves, local cold spells) often occur on local scale, but on the other hand, they are all important parts of global climate patterns which could disappear in case of a spatial data interpolation. Therefore, maps presented in this paper use similar technique applying station-based analysis.

Results of the global and European extreme climate analysis have been published in 2002–2003 (e.g., *Frich et al.*, 2002; *Klein Tank* and *Können*, 2003). In this section these results are summarized and compared for the global and continental scales. *Table 1* presents the main extreme precipitation indices that the CCl/CLIVAR task group identified and suggested for global climate extreme analysis. Beside the definition of each extreme precipitation index, *Table 1* indicates the scale (i.e., global, continental, regional) of application, as well. From the total 12 extreme climate indicators, 5, 9, and 12 were used in the analysis for the world (*Frich et al.*, 2002), Europe (*Klein Tank* and *Können*, 2003), and the Carpathian Basin (*Bartholy* and *Pongrácz*, 2004), respectively. For instance, *Figs. 1–3* present one of the extreme precipitation indices, namely, the change of the fraction of annual total rainfall due to events above the 95th percentile of daily precipitation in the baseperiod 1961–1990. Spatial distribution of global tendencies can be seen in *Fig. 1*, while the graph shown in *Fig. 2* provides the temporal details of the global mean change of the annual fraction of extreme precipitation during the second half of the 20th century. Results of the similar analysis for Europe is presented in *Fig. 3*.

Changes between the two subperiods of the second half of the century (1946–1975 and 1976–1999) have been determined during the analysis presented in *Frich et al.* (2002). The world map of *Fig. 1* indicates both the sign of change (black and grey circles for increasing and decreasing tendencies, respectively) and the magnitude of change (applying 4 different circle sizes for the percentage intervals) at each station involved in the analysis. Stations with significant changes (at 95% level of confidence) in the fraction of annual total rainfall due to events above the 95th percentile of daily precipitation in the baseperiod 1961–1990 are mapped with filled circles, while open circles indicate not significant changes. The large number of black filled circles and few grey circles on the map suggest that the annual fraction of very wet events increased between 1946 and 1999.

Based on the available time series, annual global weighted anomalies have been calculated using the baseperiod of 1961–1990. *Fig. 2* presents the annual value (in percentage) of the anomaly for the entire 1950–1999 period, as well as the fitted linear trend emphasizing the significant increasing tendency.

Table 1. Definition and indicator of extreme climate parameters

Nr.	Indicator (ECAD)	World (*Frich et al.*, 2002)	Europe (*Klein Tank* and *Können*, 2003)	Carpathian Basin (*Bartholy* and *Pongrácz*, 2004)	Definition of the extreme precipitation index	Unit
1	CDD	x		x	Maximum number of consecutive dry days (when $R_{day} < 1$ mm)	day
2	Rx1		x	x	Highest 1-day precipitation amount	mm
3	Rx5	x	x	x	The greatest 5-day rainfall total	mm
4	SDII	x		x	Simple daily intensity index (total precipitation sum / total number of days when $R_{day} \geq 1$ mm)	mm/day
5	R95T	x	x	x	Fraction of annual total rainfall due to events above the 95th percentile of the daily precipitation in the baseperiod 1961–1990 ($\Sigma R_{day} / R_{total}$, where ΣR_{day} indicates the sum of daily precipitation exceeding $R_{95\%}$)	%
6	RR10	x	x	x	Number of heavy precipitation days ($R_{day} \geq 10$ mm)	day
7	RR20		x	x	Number of very heavy precipitation days (when $R_{day} \geq 20$ mm)	day
8	R75		x	x	Number of moderate wet days ($R_{day} > R_{75\%}$, where $R_{75\%}$ indicates the upper quartile of the daily precipitation in the baseperiod 1961–1990)	day
9	R95		x	x	Number of very wet days ($R_{day} > R_{95\%}$, where $R_{95\%}$ indicates the 95th percentile of the daily precipitation in the baseperiod 1961–1990)	day
10	RR5			x	Number of precipitation days exceeding a given threshold ($R_{day} \geq 5$ mm)	day
11	RR1			x	Number of precipitation days exceeding a given threshold ($R_{day} \geq 1$ mm)	day
12	RR0.1			x	Number of precipitation days exceeding a given threshold ($R_{day} \geq 0.1$ mm)	day

The figure includes a small graph (in its upper left part) indicating the total number of stations used for the analysis each year. Except the beginning and the end of the period, about 300 stations provided valuable precipitation data to determine the annual fraction of extreme precipitation.

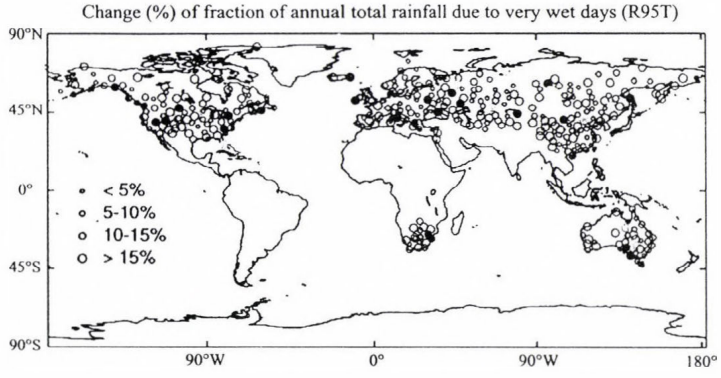

Fig. 1. Changes (%) in fraction of annual total rainfall due to events above the 95th percentile of daily precipitation in the baseperiod 1961–1990, in the second half of the 20th century. Filled circles are significant at 95% level of confidence. Grey and black indicate negative and positive changes, respectively. Circle sizes represent the magnitude of change.

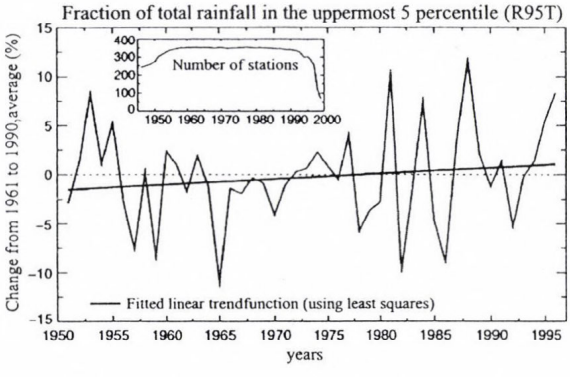

Fig. 2. Mean annual values of the fraction of annual total rainfall due to events above the 95th percentile of daily precipitation in percentage differences from the 1961–1990 weighted average values for the second half of the 20th century. The inserted graph represents the weighting factors (number of stations with valuable data) used in the linear regression analysis. The fitted linear trend is statistically significant at 95% level of confidence.

The European tendency analysis of the annual precipitation fraction due to very wet days is shown in *Fig. 3*, where the mean decadal changes of this extreme index is mapped for the stations with sufficient data for the 1946–1999

period. Open circles indicate not significant changes, while dark and grey filled circles indicate positive and negative trends, respectively. Similarly to the global analysis, significant positive tendency can be seen. According to the above results of the two large scale analyses, fraction of annual total rainfall due to events above the 95th percentile of the daily precipitation considerably increased by the end of the 20th century. Regional details of the Carpathian Basin will be presented in Section 4.

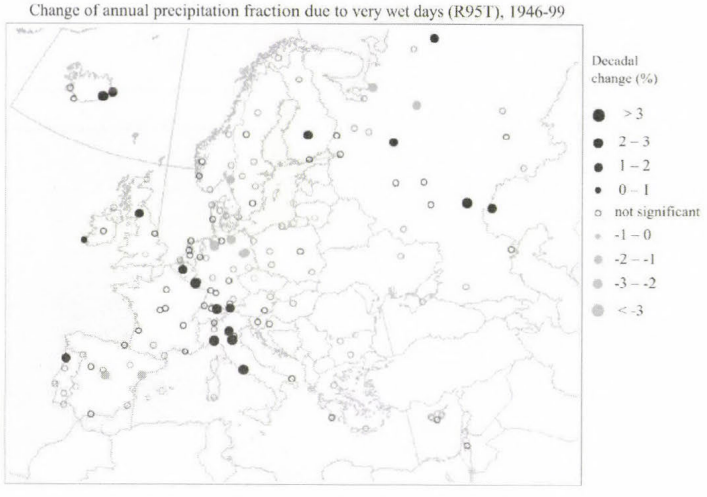

Fig. 3. Decadal trend in the fraction of annual total rainfall due to events above the 95th percentile of daily precipitation in the baseperiod 1961–1990 in Europe, for the period 1946–1999. Circles are scaled according to the magnitude of the trend. Open circles indicate not significant changes, while dark and grey filled circles indicate positive and negative trends, respectively.

Table 2 summarizes the tendencies of all extreme precipitation indices for the global and continental scale climate analyses based on the papers of *Frich et al.* (2002) and *Klein Tank* and *Können* (2003), respectively. The comparison of these results is accomplished for the second half of the last century (1946–1999). Increasing, decreasing, and not significant trends are indicated with symbols „+", „–", and „0", respectively. Considerable spatial differences are emphasized using more than one type of symbol (e.g., –/+, ++/–, +/0, etc.). After identifying the main dominant trends, exceptions are listed in case of each extreme climate index. In general, global and European tendencies are similar, and only a few small areas differ from the worldwide and continental dominant trends. Sometimes the Carpathian Basin belongs to these exceptions. For instance, both the SDII (simple daily intensity index) and the R95T

(fraction of annual total rainfall due to events above the 95th percentile of the baseperiod) are dominantly increasing for the world, as well as for Europe. However, for the Carpathian Basin neither the global, nor the continental scale analysis include significant trends. One of the aims of our research presented in this paper is to specify these cases on a finer spatial scale and provide more details for Hungary and the surrounding region. The next sections contain our results.

Table 2. Comparison of the tendencies of extreme climate indices based on global (*Frich et al.*, 2002) and European (*European Climate Assessment & Dataset* (ECAD) project; *Klein Tank* and *Können*, 2003) extreme analysis for the period 1946–1999

Nr.	Extreme index	World (*Frich et al.*, 2002)	Europe (*Klein Tank* and *Können*, 2003)
1	CDD Consecutive dry days	– / + Negative tendency dominates except the eastern part of Asia	**0** No significant trend
2	Rx1 Highest 1-day precipitation amount	No analysis provided	+ / – Positive tendency dominates in Western and Northern Europe, while negative tendency dominates in Eastern and Southern Europe
3	Rx5 Greatest 5-day rainfall total	+ / – Positive tendency dominates except the eastern part of Asia	+ / – Positive tendency dominates except Central and Southern Europe
4	SDII Simple daily intensity index	+ / – Positive tendency dominates except Asia	+ / **0** Positive tendency dominates in Western and Northern Europe, while no significant trend can be observed at other places
5	R95T Fraction of annual total rainfall due to events above the 95th percentile	+ / – Positive tendency dominates except Asia	+ / **0** Positive tendency dominates in Northern Europe and the Alpes, while no significant trend can be observed at other places
6	RR10 Heavy precipitation days	+ + / – Positive tendency dominates except the eastern part of Asia	+ / – Positive tendency dominates except Central and Southeastern Europe
7	RR20 Very heavy precipitation days	No analysis provided	+
8	R75 Moderate wet days	No analysis provided	+ + / – Positive tendency dominates except Central and Southern Europe
9	R95 Very wet days	No analysis provided	+

3. Comparison of tendencies of extreme precipitation indices for the Carpathian Basin and Europe

In order to evaluate the past and future climate tendencies of the Carpathian Basin, it is essential to compare regional tendencies of the different climate parameters to larger (i.e., continental) scale.

Giorgi and *Francisco* (2000) analyzed the future continental temperature and precipitation changes expected for the 21st century based on model outputs of five main AOGCMs (Atmosphere-Ocean General Circulation Model). Global continental areas were divided into 23 regions, from which 2 cover the European continent, namely, (i) Northern Europe (NEU), and (ii) the Mediterranean region (MED).

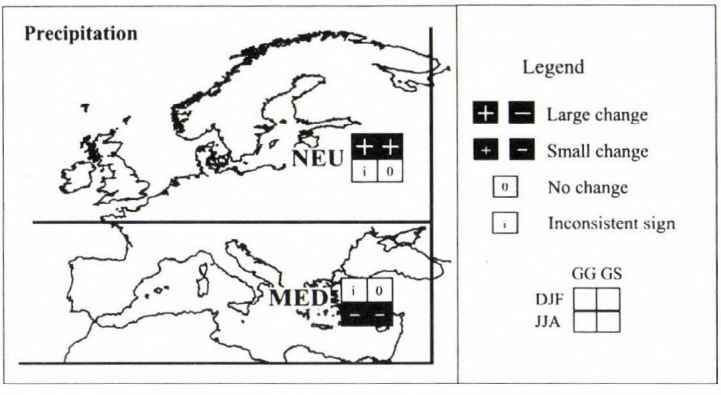

Fig. 4. Summary of precipitation tendency analysis for Northern Europe (NEU) and the Mediterranean region (MED) for two seasons (winter and summer) and two climate scenarios (GG, GS) based on inter-model consistency analysis of *Giorgi* and *Francisco* (2000).

Fig. 4 summarizes intensity, sign, and consistency of the GCM-based precipitation changes for these two European regions. Expected changes in precipitation conditions are presented in four small boxes for NEU and MED for 2071–2100. The upper and the lower two boxes represent expected changes in winter (December–January–February), and in summer (June–July–August), respectively. Furthermore, results for the GG (greenhouse gas only case) and GS (greenhouse gas with increasing sulphate aerosol case) scenario are shown in the left two boxes, and in the right two boxes, respectively. "+" and "–" signs appearing in the small boxes indicate the intensity of precipitation change compared to the baseperiod 1961–1990. Similarly, black and grey colors imply large (greater than 20%) and small (between 5% and 20%) average change, respectively. "0" indicates no change (between –5% and +5%), while in case

of model disagreement, sign of inconsistency ("i") appears in the small box. Results of *Giorgi* and *Francisco* (2000) suggest that winters in Northern Europe are tend to become considerably wetter, and Mediterranean summers are likely to become drier than today for both GG and GS scenarios. Estimations of the five main AOGCMs are inconsistent for NEU summers and MED winters for the GG scenario, while they do not indicate significant changes for the GS scenario.

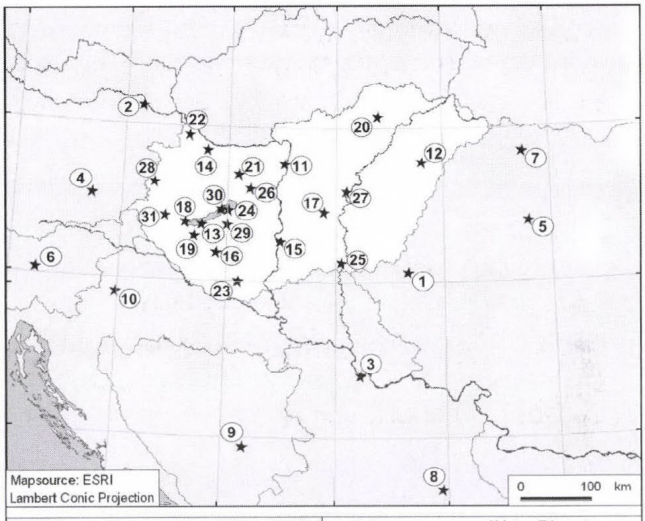

Station	N.lat.	E.long.	m
Stations in neighbouring countries			
1 Arad	46°08'	21°21'	117
2 Vienna	48°14'	16°21'	199
3 Beograd	44°48'	20°28'	132
4 Graz	47°05'	15°27'	366
5 Cluj Napoca	46°47'	23°34'	410
6 Ljubljana	46°04'	14°31'	299
7 Baia Mare	47°40'	23°30'	216
8 Nis	43°20'	21°54'	202
9 Sarajevo	52°30'	22°30'	211
10 Zagreb	45°49'	15°59'	157
Hungarian stations			
11 Budapest	47°31'	19°02'	118
12 Debrecen	47°33'	21°37'	123
13 Fonyód	46°44'	17°33'	166
14 Győr	47°41'	17°38'	119
15 Kalocsa	46°31'	18°59'	92
16 Kaposvár	46°22'	17°50'	152
17 Kecskemét	46°54'	19°46'	114
18 Keszthely	46°45'	17°15'	115
19 Marcali	46°35'	17°25'	128
20 Miskolc	48°08'	20°48'	118
21 Mór	47°23'	18°12'	203
22 Mosonmagyaróvár	47°53'	17°16'	121
23 Pécs	46°00'	18°14'	202
24 Siófok	46°55'	18°02'	108
25 Szeged	46°15'	20°06'	82
26 Székesfehérvár	47°12'	18°25'	111
27 Szolnok	47°10'	20°12'	90
28 Szombathely	47°15'	16°38'	218
29 Tab	46°44'	18°01'	177
30 Tihany	46°55'	17°54'	150
31 Zalaegerszeg	46°50'	16°51'	162

Fig. 5. Geographical locations of meteorological stations in the Carpathian Basin.

Tendency analysis of precipitation extreme indices for the last century is presented in this section for the Carpathian Basin, and compared to the results of the European analysis based on *Klein Tank* and *Können* (2003). For the evaluation of recent tendency of precipitation extremes in the Carpathian Basin, 31 meteorological stations have been used (*Fig. 5*). Datasets for the 21

Hungarian stations were bought from the Hungarian Meteorological Service, while datasets for the 10 stations in the neighbouring countries are freely available via Internet from ECAD (*Klein Tank*, 2003). Stations have been selected considering two main criteria, namely, (i) homogeneous spatial coverage, and (ii) minimal number of missing data. However, none of these criteria could be fulfilled absolutely. *Fig. 6* presents the relative number of missing data for each station using two concentric circles. In front of the grey circles indicating missing data for the entire 20th century, black circles represent missing data ratio for the second half of the century. Annual total numbers of meteorological stations with valuable precipitation data are shown for Hungary, for the neighbouring countries, and for the entire Carpathian Basin in *Fig. 7*. Obviously, in the first half of the century the database contains much less information available than in the second half.

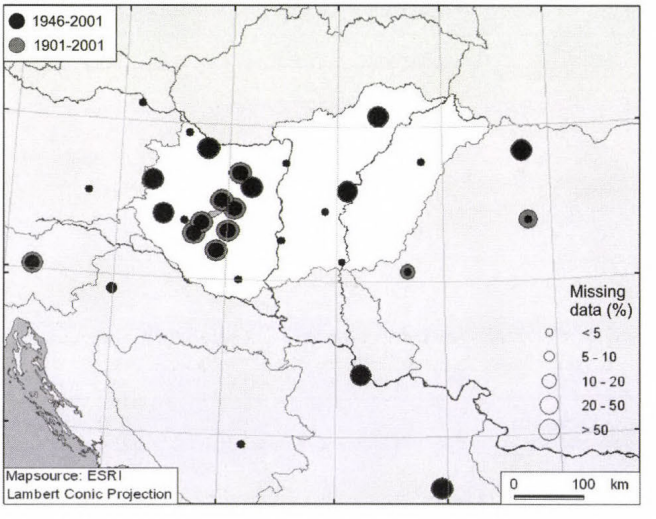

Fig. 6. Fraction of missing data during 1901–2001 (grey circles) and 1946–2001 (black circles).

Our datasets are compiled for 1901–2001. However, based on previous analyses (*IPCC*, 2001) suggesting that precipitation and temperature tendencies of the last quarter of the 20th century and the second half of the century are significantly different, and due to the limited extent of the European time series (*Klein Tank et al.*, 2002a; *Klein Tank* and *Können,* 2003), the European-Carpathian comparison has been accomplished for 1946–2001 and 1976–2001. *Table 3* summarizes the spatial structures of decadal tendency maps for the 12 extreme precipitation indices for both periods. When similar changes are detected for all stations appearing on the map, only one "+" or "–" sign

indicates the tendency. While in case of more complex spatial structures, two or four signs have been used to illustrate the regional tendencies. The intensity of the changes is represented by three categories (i.e., weak, medium, strong). Based on the analysis of tendency maps, only very few extreme indices can be characterized by homogeneous positive or negative trends in both periods and for both regions. However, in general, the precipitation extremes decreased slightly in the Carpathian Basin during the last 56 years, while they increased more intensely during the last 26 years. Opposite tendencies can be observed in the entire European continent, namely, increased and decreased extreme precipitation trends in the second half and in the last quarter of the century, respectively.

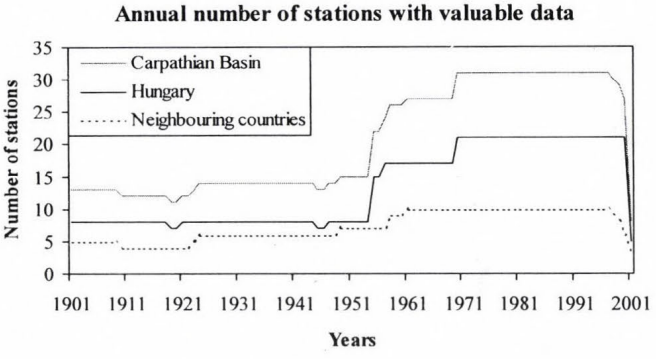

Fig. 7. Annual total number of meteorological stations of the Carpathian Basin with valuable precipitation data (1901–2001).

In this paper two parameters of *Table 3* are presented in details. European and Carpathian tendencies of annual number RR10 of heavy precipitation days (when daily precipitation is greater than 10 mm) are compared for the last quarter of the 20th century in *Fig. 8.* Circles represent decadal trend coefficients of the meteorological stations (using the baseperiod 1961–1990). Black and grey circles indicate increasing and decreasing tendencies, respectively, while circle size depends on the intensity of these positive or negative trends. Based on the tendency analysis of the entire European continent (upper panel of *Fig. 8*), heavy precipitation days occurred more often in the last 2–3 decades in northern stations, while they became less frequent in the Mediterranean region. The Carpathian Basin is located in-between, however, our detailed regional analysis (lower panel of *Fig. 8*) suggests that except a few southern stations, the annual number of heavy precipitation days (RR10) increased during the last 26 years.

Table 3. Summary of tendency analyses of extreme precipitation indices for the Carpathian Basin (*Bartholy* and *Pongrácz*, 2004) and Europe (based on *ECAD*, *Klein Tank*, 2003; *Klein Tank* and *Können*, 2003) for the 1946–2001 and for the 1976-2001 periods

Nr.	Extreme index	Carpathian Basin		Europe	
		1946-2001	1976-2001	1946-1999	1976-1999
1	CDD Consecutive dry days	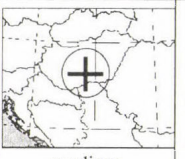 medium	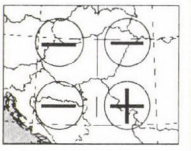 strong	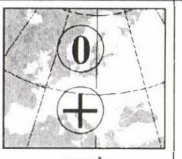 weak	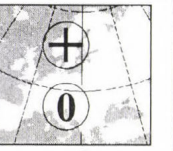 weak
2	Rx1 Highest 1-day precipitation amount	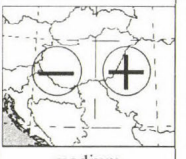 medium	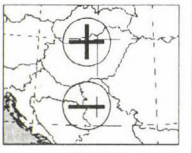 strong	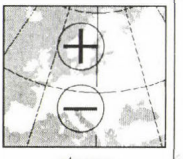 strong	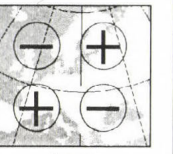 strong
3	Rx5 Greatest 5-day rainfall total	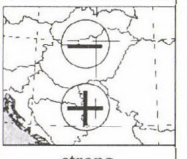 strong	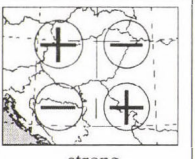 strong	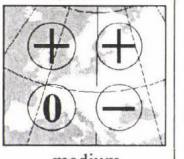 medium	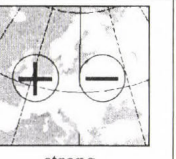 strong
4	SDII Simple daily intensity index	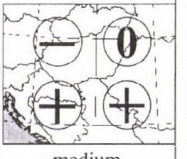 medium	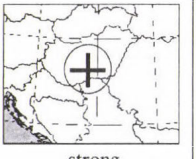 strong	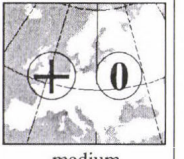 medium	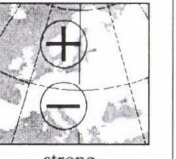 strong
5	R95T Fraction of annual total rainfall due to events above the 95th percentile	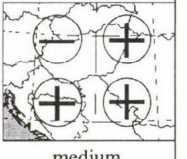 medium	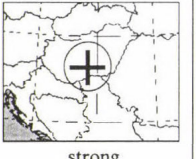 strong	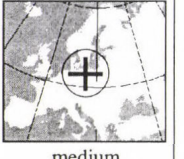 medium	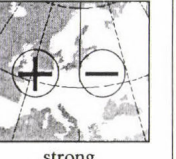 strong
6	RR10 Heavy precipitation days	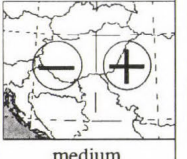 medium	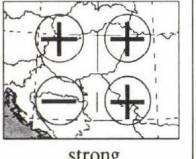 strong	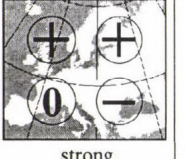 strong	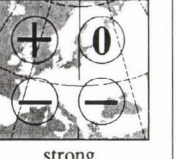 strong

→

7	RR20 Very heavy precipitation days	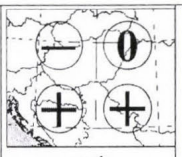 weak	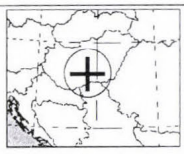 strong	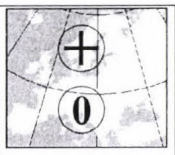 medium	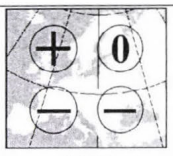 strong
8	R75 Moderate wet days	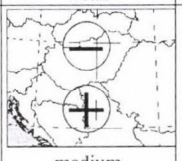 medium	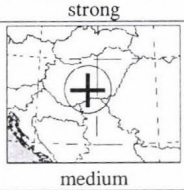 medium	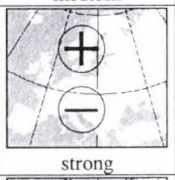 strong	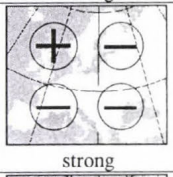 strong
9	R95 Very wet days	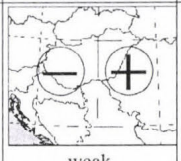 weak	 strong	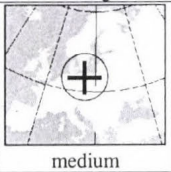 medium	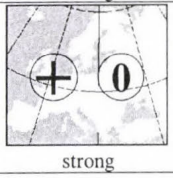 strong
10	RR5 Precipitation days exceeding 5 mm	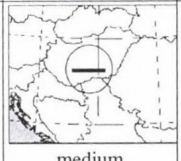 medium	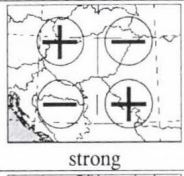 strong	No analysis available	No analysis available
11	RR1 Precipitation days exceeding 1 mm	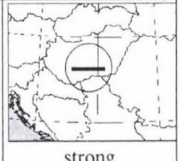 strong	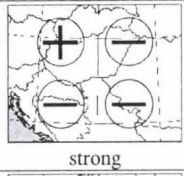 strong	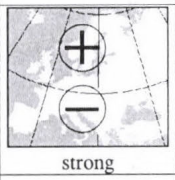 strong	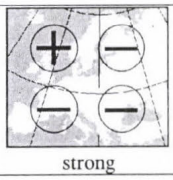 strong
12	RR0.1 Precipitation days exceeding 0.1 mm	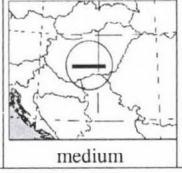 medium	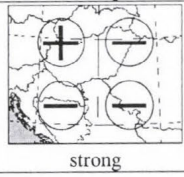 strong	No analysis available	No analysis available

Indices listed in *Table 1* include a few precipitation-related parameters which do not indicate extreme conditions. They belong to the index type *annual number of precipitation days exceeding a given threshold*, for instance, RR1 is one of them. Decadal tendency of the annual number of wet days with daily precipitation exceeding 1 mm (RR1) is analyzed for the second half of the 20th century (*Fig. 9*). Similarly to *Fig. 8*, the upper two maps compare spatial distribution of decadal trends for the European continent and the Carpathian Basin, while the lower graph shows the regional mean time series of the RR1 anomalies (using the baseperiod 1961–1990) for the Carpathian

Basin only. The small graph in the upper right part illustrates the number of stations used for calculating the spatial average. For Europe, similarly to RR10, considerable zonal pattern can be recognized, namely, positive trends in the northern regions, while negative trends in the southern part. For the Carpathian Basin decadal tendency of RR1 is strongly negative in the last 56 years in most of the stations, as well as in case of the regional mean anomaly.

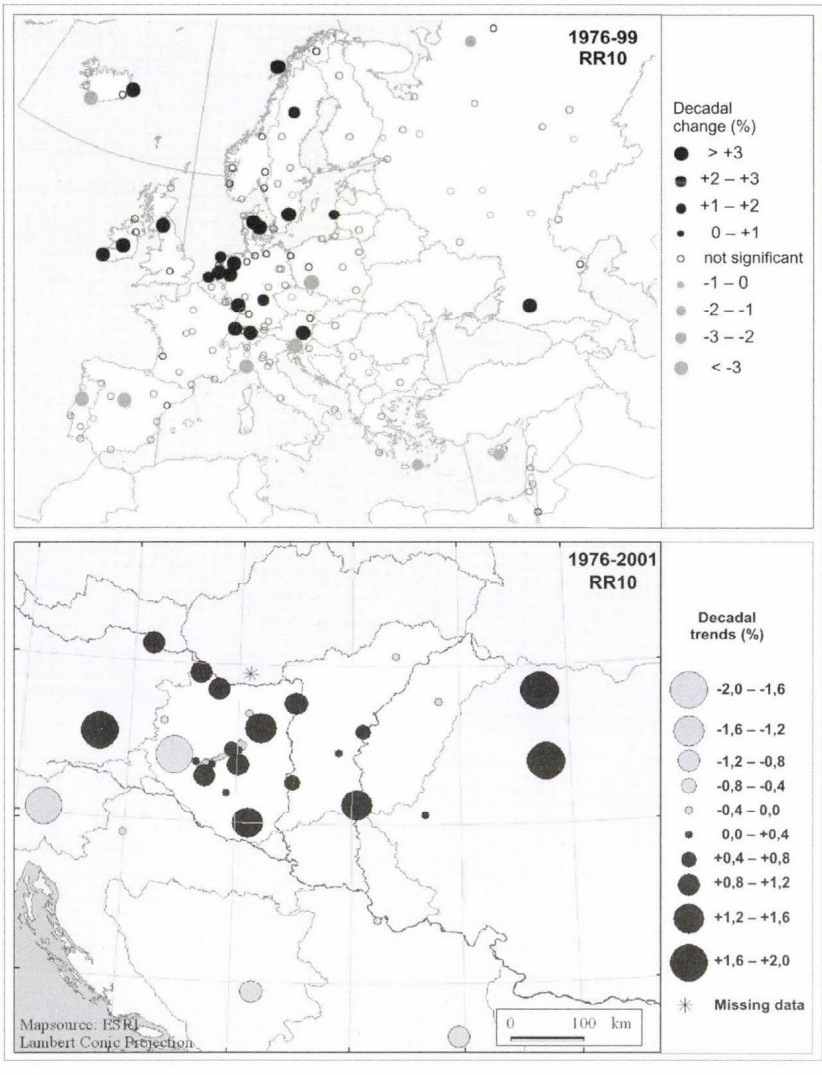

Fig. 8. Tendency of annual number of heavy precipitation days exceeding 10 mm (RR10) in Europe and the Carpathian Basin during the last quarter of the 20th century. Trend coefficients of the Carpathian Basin greater than 0.4 in absolute value are significant at 95% level of confidence.

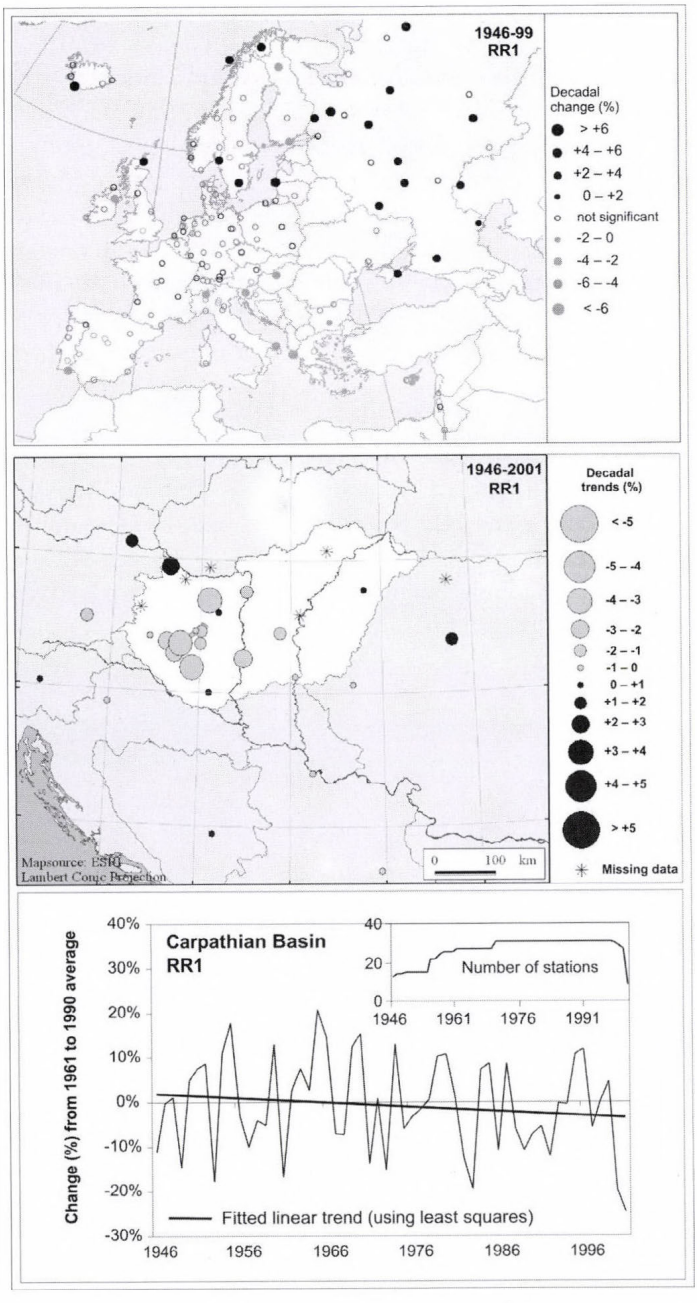

Fig. 9. Tendency of annual number of precipitation days exceeding 1 mm (RR1) in Europe and the Carpathian Basin during the second half of the 20th century. Trend coefficients of the Carpathian Basin greater than 0.3 in absolute value are significant at 95% level of confidence.

4. Analysis of extreme precipitation indices for the Carpathian Basin

According to the *IPCC TAR* (2001), climate and agriculture of several regions of the world can be strongly affected by increasing occurrence of precipitation extremes in the 21st century. Based on the information of the 44 small maps presented in *Table 3*, most of the extreme precipitation indices increased considerably in the Carpathian Basin by the end of the 20th century. Positive trends were detected mostly in the last 26 years. The strongest increasing tendencies appear in case of extreme indices indicating very intense or large precipitation (i.e., SDII, R95T, RR20, RR75, R95). Similar results were concluded in *Bartholy* and *Pongrácz* (1998), *Pongrácz* and *Bartholy* (2000), and *Bartholy et al.* (2003).

In this section, spatial distribution maps of tendency of extreme precipitation indices changed the most are presented in *Figs. 10–12*. Decadal changes of annual number of very heavy precipitation days (RR20) are illustrated in *Fig. 10* for the last 26 years (1976–2001). The entire Carpathian Basin can be characterized by a strong positive trend. Considering only the Hungarian stations, the annual number of wet days exceeding 20 mm increased more in Transdanubia than in the Great Plains.

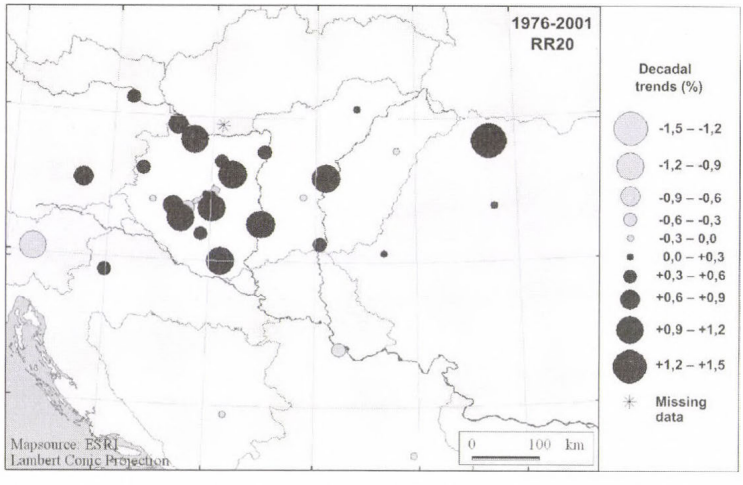

Fig. 10. Tendency of annual number of very heavy precipitation days exceeding 20 mm (RR20) in the Carpathian Basin during the last quarter of the 20th century. Trend coefficients greater than 0.3 in absolute value are significant at 95% level of confidence.

Fig. 11 compares the tendency of annual rainfall fraction due to very wet days (R95T) during the second half and the last quarter of the 20th century. Slight decreasing tendencies can be detected in the Transdanubian stations

during 1946–2001, while intermediate positive trends appear in other stations of the region on the left map of the figure. Furthermore, very strong positive trends were found during the last 26 years (shown on the right map) indicating that the annual fraction of total rainfall (R_{total}) due to events above the 95th percentile ($R_{95\%}$) of daily precipitation in the baseperiod 1961–1990 ($\Sigma R_{day}/R_{total}$, where ΣR_{day} indicates the sum of daily precipitation exceeding $R_{95\%}$) increased significantly between 1976 and 2001.

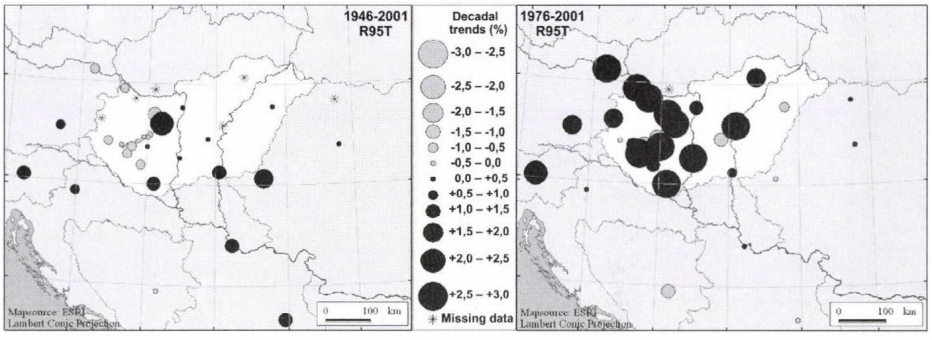

Fig. 11. Tendency of fraction of total annual rainfall due to very wet days (R95T) in the Carpathian Basin. Trend coefficients greater than 0.3 and 0.4 in absolute value are significant at 95% level of confidence on the left and right map, respectively.

Finally, tendency analysis of RR0.1 (annual number of precipitation days exceeding 0.1 mm) for the second half of the 20th century for the Carpathian Basin is presented in *Fig. 12.* Although, according to the definition, this parameter does not refer to extreme precipitation events, in order to accomplish a complex analysis of precipitation conditions in the Carpathian Basin, several indices defined as numbers of precipitation days exceeding a given threshold (i.e., 20 mm, 10 mm, 5 mm, 1 mm, 0.1 mm) were included.

The upper two maps compare annual tendency of RR0.1 for the last 56 years (on the left) and the last 26 years (on the right). Seasonal tendencies of RR0.1 are compared for the last quarter of the 20th century on the lower two maps (winter and summer trends are presented on the left and right map, respectively). All these maps indicate intermediate or strong negative trends, the strongest trends occur in case of annual RR0.1 values between 1976 and 2001, when both increasing and decreasing tendency appeared in the Transdanubian region. Furthermore, negative trends in winter (on the lower left map) exceed summer trends (on the lower right map).

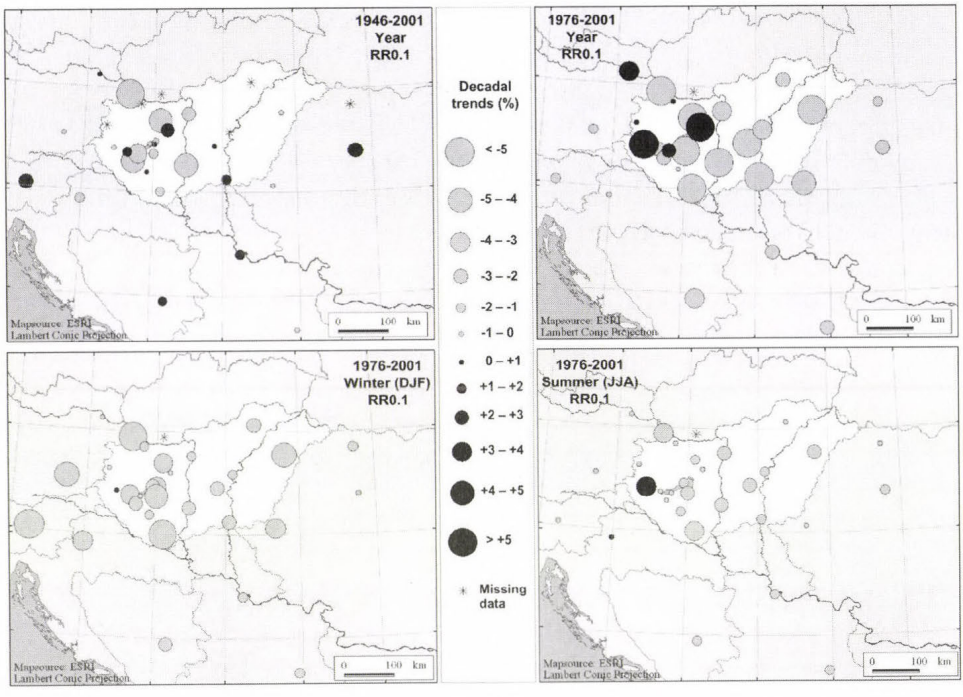

Fig. 12. Tendency of annual number of precipitation days exceeding 0.1 mm (RR0.1) in the Carpathian Basin. Trend coefficients greater than 0.3 (on the upper left map) and 0.4 (on the other three maps) in absolute value are significant at 95% level of confidence.

Summarizing the results presented in *Figs. 11* and *12*, these analyses can be concluded that although, in general, precipitation occurred more rarely in the Carpathian Basin, the ratio of heavy or extreme precipitation days increased considerably by the end of the 20th century.

5. Conclusions

Based on the analysis of extreme precipitation indices for the second half of the 20th century presented in this paper, the following conclusions can be drawn.

1. Comparison of the global and European tendency resulted in:

   (i) Positive trends dominate in both analyses in case of Rx5, SDII, R95T, and RR10. Opposite (i.e., negative) trends occurred in Asia and Central/Southeastern Europe.

(ii) Most of the European continent can be characterized by increasing tendency of indices Rx1 and R75, while decreasing tendency was found only in Central and Southeastern Europe. Global analysis is not available for these indices.

(iii) In case of RR20 and R75, significant positive trend appeared in Europe (global analysis is not available for these indices).

(iv) Global decreasing (except Eastern Asia) tendency of CDD implies similar climate conditions to the consequent trends of extreme precipitation indices listed above. However, trends are not significant for the European continent.

2. Comparison of the analysis for Europe and the Carpathian Basin:

(i) Decadal trends were evaluated separately for two periods (1946–2001 and 1976–2001). Tendencies in both the European and Carpathian regions were more intense and spatially more homogeneous during the last 26 years than the last 56 years.

(ii) Spatial structure of the decadal tendency maps is classified into several main patterns using one, two (meridionally or horizontally), or four "+" or "–" signs. Considerable zonal patterns were often recognized in Europe, when different tendency occurred in Northern Europe and the Mediterranean region.

3. Analysis of the extreme precipitation indices for the Carpathian Basin (according to the suggestions of the CCl/CLIVAR Working Group):

(i) Strong positive trends were detected in most of the extreme precipitation indices (e.g., SDII, R95T, RR20, R75, R95) for the last quarter of the 20th century indicating increasing precipitation extremity in the Carpathian Basin.

(ii) Significant negative trends dominate the region in case of the non-extreme parameters (i.e., RR5, RR1, and RR0.1) during the second half of the 20th century.

(iii) In general, precipitation occurred less frequently in the Carpathian Basin, however, the ratio of heavy or extreme precipitation days increased considerably by the end of the 20th century.

Acknowledgements–Research leading to this paper has been supported by the Hungarian National Science Research Foundation (OTKA) under grants T-026629, T-034867, and T-038423, also by the AEROCARB and CHIOTTO projects of the European Union Nr. 5 program under grants EVK2-CT-1999/0013, EVK2-CT-2002/0163, the Hungarian National Research Development Program under grant NKFP-3A/0006/ 2002, and VAHAVA project of the Hungarian Academy of Sciences and the Ministry of Environment and Water. ESRI software has been used to create maps. Furthermore, supports of the Bolyai János Research Fellowship of the Hungarian Academy of Sciences is appreciated.

References

Bartholy, J. and *Pongrácz, R.*, 1998: The differing trends of the Hungarian precipitation time series, areal and decadal changes of extreme precipitation (in Hungarian). In *Second Conference on Forest and Climate* (eds.: *K. Tar* and *K. Szilágyi*). Kossuth Egyetemi Nyomda, Debrecen, 62-66.

Bartholy, J. and *Pongrácz, R.*, 2004: *Global and regional tendencies of extreme indices based on daily precipitation for the 20th century* (in Hungarian). Research Paper. Eötvös Loránd Tudományegyetem, Budapest. 20p.

Bartholy, J., Pongrácz, R., Matyasovszky, I., and *Schlanger, V.*, 2003: Expected regional variations and changes of mean and extreme climatology of Eastern/Central Europe. In *Combined Preprints CD-ROM of the 83rd AMS Annual Meeting*. American Meteorological Society, Boston. Paper 4.7, 10p.

Easterling, D.R., Meehl, G.A., Parmesan, C., Chagnon, S.A., Karl, T., and *Mearns, L.O.*, 2000: Climate extremes: Observation, modelling and impacts. *Science 289*, 2068-2074.

Folland, C.K., Frich, P., Rayner, N., Basnett, T., Parker, D.E., and *Horton, B.*, 2000: Uncertainities in climate datasets: A challenge for WMO. *WMO Bulletin 49*, 59-68.

Frich, P., Alexander, L.V., Della-Marta, P., Gleason, B., Haylock, M., Klein Tank, A.M.G., and *Peterson, T.*, 2002: Observed coherent changes in climatic extremes during the second half of the twentieth century. *Climate Res. 19*, 193-212.

Giorgi, F. and *Francisco, R.*, 2000: Evaluating uncertainties in the prediction of regional climate change. *Geophys. Res. Lett. 27*, 1295-1298.

IPCC, 2001: *Climate Change 2001: Third Assessment Report. The Scientific Basis*. Cambridge University Press, Cambridge, UK.

IPCC, 1995: *Climate Change 1995: The Science of Climate Change. Contribution of Working Group I to the Second Assessment of the Intergovernmental Panel on Climate Change*. Cambridge University Press, Cambridge, UK.

Karl, T.R., Nicholls, N., and *Ghazi, A.*, 1999: Clivar/GCOS/WMO Workshop on Indices and Indicators for Climate Extremes Workshop Summary. *Climatic Change 42*, 3-7.

Klein Tank, A.M.G., 2003: *The European Climate Assessment and Dataset Project*. http://www.knmi.nl/samenw/eca/index.html.

Klein Tank, A.M.G., and *Können, G.P.*, 2003: Trends in indices of daily temperature and precipitation extremes in Europe, 1946-99. *J. Climate 16*, 3665-3608.

Klein Tank, A.M.G., and *Coauthors*, 2002a: Daily dataset of 20th-century surface air temperature and precipitation series for the European Climate Assessment. *Int. J. Climatol. 22*, 1441-1453.

Klein Tank, A.M.G., Wijngaard, J.B., and *van Engelen, A.*, 2002b: *Climate of Europe; Assessment of observed daily temperature and precipitation extremes*. KNMI, De Bilt, The Netherlands, 36p.

Nicholls, M., Gruza, G.W., Jouzel, J., Karl, T.R., Ogallo, L.A., and *Parker, D.E.*, 1996: Chapter 3, Observed climate variability and change. In *Climate Change 1995: The Science of Climate Change. Contribution to Working Group I to IPCC SAR*. (eds.: *J.T. Houghton et al.*) Cambridge Univ. Press, 137-192.

Peterson, T.C. and *Vose, R.S.*, 1997: An overview of the global historical climatology network database. *B. Am. Meteorol. Soc. 78*, 2837-2849.

Peterson, T., Folland, C.K., Gruza, G., Hogg, W., Mokssit, A., and *Plummer, N.*, 2002: Report on the Activities of the Working Group on Climate Change Detection and Related Rapporteurs, 1998-2001. *World Meteorological Organization Rep. WCDMP-47. WMO-TD 1071*. Geneva, Switzerland. 143p.

Pongrácz, R. and *Bartholy, J.*, 2000: Changing trends in climatic extremes in Hungary. In *Third Conference on Forest and Climate* (ed.: *A. Kircsi*). Kossuth University Press, Debrecen, 38-44.

Trewin, B.C., 1999: The development of a high-quality daily temperature datasets for Australia and implications for the observed frequency of extreme temperatures. In *Meteorology and Oceanography at the Millenium: AMOS'99 Proc. of the 6th National Australian Meteorological and Oceanographic Society Congress*, Canberra, 1999, pp. 87.

IDŐJÁRÁS

Quarterly Journal of the Hungarian Meteorological Service
Vol. 109, No. 1, January–March 2005, pp. 21–37

Microclimate simulation in maize with two watering levels

Angéla Anda* and **Zsuzsanna Lőke**

University of Veszprém, Georgikon Faculty of Agronomy,
P.O. Box 71, H-8361 Keszthely, Hungary; E-mail:anda-a@georgikon.hu

(Manuscript received in final form January 6, 2005)

Abstract—Various components in the microclimate of irrigated and rainfed maize stands were examined in Keszthely, Hungary, from the end of June 2001 until the first ten days of August. To simulate the elements of microclimate, Crop Microclimate Simulation Model of *Goudriaan* (1977) was applied. The air temperature and humidity were registered using a Temperature/Relative Humidity Sensor, attached to a data recorder placed in a Stevenson screen, close to the tassel level of the adult plants (1.40 m above the soil surface). Measured and simulated values were compared with respect to hourly means of samples taken every 4 seconds, and diurnal means calculated for the daylight hours. The weather on certain sampling days (rain and strong winds) resulted in a microclimate simulation so far from reality, that these days were omitted from the evaluation. The difference between the diurnal means of simulated sampling days and the measured values was small, less than 1 °C for the air temperature, and below 10% for the relative humidity. The simulation of air temperature was closer to the field parameters in the non-irrigated treatment. The difference between the observed and simulated air moisture values was much the same in the two water supply treatments. The microclimate simulated was such a good approximation to reality that the simulation was able to reflect events causing very slight differences, such as the effect of irrigation. This indicates that a knowledge of the changes in the microclimate, expected as the result of various agronomic measures, could form the basis for better decisions by farmers.

Key-words: Goudriaan microclimate-simulation, maize, irrigation, CWSI

1. Introduction

The most widely-used model for the simulation of maize production is the CERES-Maize model (*Jones* and *Kiniry,* 1986), which has been modified and improved by many authors, including *Stockle* and *Kiniry* (1990), *Kiniry* and

* Corresponding author

Knievel (1995), *Kiniry et al.* (1997), *Kiniry* and *Bockholt* (1998), and *Xie et al.* (2001). The model has been applied under a wide variety of climatic conditions (*Carberry et al.*, 1989; *Liu et al.*, 1989; *Plantureaux et al.*, 1991; *Nouna et al.*, 2001). *Mantovani et al.* (1995) and *Cavero et al.* (2001) combined the CERES model with the CROPWAT irrigation model in order to give a more precise description of yield variability. The spatial variability in yield caused by yield losses in crop patches exposed to various stress factors was numerically determined by *Paz et al.* (1998). During the past decade, the CERES model was applied by *Huzsvay* and *Nagy* (1994), and by *Fodor et al.* (2003) for yield simulation purposes. The soil-vegetation-atmosphere transfer schemes, as for example SVAT, produce another important and popular model category (*Franks et al.*, 1997; *Calveta et al.*, 1998; *Calveta,* 2000; *Gottschalk et al.*, 2001).

Probably due to the limited number of users, none of the microclimate models is applied on such a wide global scale as the above-mentioned models. In Europe, *Goudriaan* (1977) compiled a model for the simulation of the maize microclimate, which was simplified by *Chen* (1984) and adapted for PC application, thus broadening the range of possible users. The model was based on the synthesizing work of many other authors (*Sellers,* 1965; *Evans,* 1972; *Nobel,* 1974; *Rosenberg,* 1974; *de Wit* and *Goudriaan* 1978; etc.). Research continued after the publication of the model, and *Jones* (1983) published a comprehensive work on plant microclimates, which could be regarded as a theoretical manual. The latest results about the Goudriaan's model "team-work" appeared in 1994 (*Goudriaan* and *van Laar,* 1994).

Before applying the Goudriaan model in the present work, further slight modifications were made, which facilitated its application without affecting the basic structure of the model (*Anda et al.*, 2001).

Research on the use of plant temperatures to determine irrigation dates began in the early '80s, in two separate directions. One is linked with the work of *Jackson et al.* (1981), and involves the determination of a water stress index with a strong theoretical basis, while the other involves the formation of a water stress index on a largely empirical basis, the first work on which was published by *Idso et al.* (1981). The advantages of estimating the water status of maize on the basis of plant temperature were discussed among others by *Gardner et al.* (1981), *Hatfield* (1990), and *Irmak et al.* (2000).

The aim of the present paper was to control the Goudriaan simulation model (CMSM, Crop Microclimate Simulation Model) for the microclimate of maize grown under rainfed conditions, or with irrigation based on the real water requirements of the plant. Although the effect of irrigation on the plant microclimate has long been known, the more exact measurements of air temperature and humidity, made possible by developments in instrumental

techniques, justify a new look at the microclimate modifications occurring as the result of supplementary water supplies. The exact value of air temperature is important in plant studies, because it governs physiological processes. The humidity of the air determines the appearance of some plant diseases. Modeling could provide a basis for a better understanding of the microclimatic differences arising as the result of various human interventions such as irrigation. A more detailed knowledge of the microclimate of irrigated plants could also be of importance in farm practice (e.g., through the consideration of environmental conditions in controlling the spread of plant diseases). The sophisticated consideration of the elements of microclimate could provide better understanding of the processes near the plants. The investigations did not aim to compare the well known microclimates of irrigated and non-irrigated plant stands; these treatments were used only to achieve two different levels of water supplies.

2. Materials and methods

The experiment was set up at the Agrometeorological Research Station in Keszthely, during the 2001 growing season, using a widely cultivated, Hungarian-bred maize hybrid with a short vegetation period (Gazda, FAO 400, dent variety, prolific and tolerant of water stress). The typical soil type on this area was Ramann's brown forest soil (*Anda* and *Stephens,* 1996).

Plants sown in late April emerged during the first ten days of May, after which the plant density was adjusted to 7 plants/m^2. The usual agronomic measures (plant protection, weed control), recommended for the location by the staff of Keszthely University of Agricultural Sciences, were applied. Nutrients (100 kg ha^{-1} N, 80 kg ha^{-1} P and 120 kg ha^{-1} K) were applied in spring immediately prior to sowing. Harvesting was carried out in late September.

The plots measured 0.25 ha, and were arranged in blocks to facilitate the placement of the trickle irrigation pipes. The irrigation dates were determined on the basis of the crop water stress index (CWSI) calculated from differences in the plant and air temperatures and humidity. This index is based on the heat balance, transformed to a certain extent using diffusion resistance values (r_c: crop resistance (s m^{-1}), r_a: aerodynamic resistance (s m^{-1}), subscript p designates unlimited water supplies), giving:

$$CWSI = \frac{\gamma\,(1 + r_c / r_a) - \gamma}{\Delta + \gamma\,(1 + r_{c\,p} / r_a)}, \tag{1}$$

where γ is psychrometric constant (Pa K^{-1}),

Δ is slope of saturated vapor pressure-temperature relation (Pa K^{-1}).

In the calculation of the index, a central parameter formed from the difference between the plant canopy and air temperatures (T_c–T_a) is an important factor when expressing the resistances:

$$r_c / r_a = \frac{\gamma\, r_a R_n /(\rho c_p) - (T_c - T_a)(\Delta + \gamma) - [e_s(T_c) - e]}{\gamma[(T_c - T_a) - r_a R_n /(\rho c_p)]}, \qquad (2)$$

where R_n: net radiation (W m^{-2}),

$e(T_c) - e$: difference between saturation and actual vapor concentrations of the air (Pa),

ρ: air density (kg m^{-3}),

c_p: specific heat capacity of the air at constant pressure (J kg^{-1} K^{-1}).

For details of the CWSI determination, see *Jackson* (1982).

The most important plant parameter in this index is the diurnal plant surface (canopy) temperature (T_c), which could be measured after canopy closure only, under unclouded conditions when the sun was high in the sky. The RAYNGER II.RTL infra-thermometer was held approximately 1 m above the plant stand at an angle of 30° to the horizontal, assuming an emission factor of 0.96.

Irrigation was applied at higher rates (55–60 mm) at the beginning and end of the vegetation period to counteract the substantial water deficiency, while lower rates (20–30 mm) were applied in the intervening periods. Irrigation was carried out when the CWSI value exceeded 0.25. This limit value was determined on the basis of 12 years of maize irrigation experiments carried out locally (*Anda,* 1993; *Anda et al.,* 2001).

The LAI was measured on the same 10 sample plants for each treatment weekly, using the LI-3000A type leaf-area-meter. The model divides the whole canopy into homogeneous layers. The number of layers depends on the actual structure of the plant stand.

Among the components of the microclimate, the air temperature and air humidity were recorded between June 29 and August 6 with a Temperature/Relative Humidity Sensor connected to an LI-1000 DataLogger housed in a Stevenson screen. The instrument shelter was placed at 1.40 m above the soil surface. In the first half of the experiment the sensor was placed in the non-irrigated control stand, but later it was transferred to the irrigated stand. The limited equipment availability did not make it possible to quantify the effect of irrigation by carrying out parallel observations. The time of investigation was chosen after canopy closure, when the environmental conditions are the most suitable for microclimate measurements. The duration of the study was in accordance with the time periods of model constructers applied during the controlling process of the model (*Goudriaan,* 1977).

The theory of the CMSM is the calculation of the radiation distribution among different environmental processes. The sensible heat flux (H_i) in the ith layer is:

$$H_i = \rho c_p \frac{T_{ci} - T_{ai}}{r_{aHi}}, \tag{3}$$

where T_{ai}: air temperature in the ith layer (K),

T_{ci}: air temperature in the ith layer (K),

r_{aHi}: aerodynamic resistance for sensible heat transfer in the ith layer (s m^{-1}).

The latent heat flux (λE_i) in the ith layer can be calculated as follows:

$$\lambda E_i = \rho c_p \{e_s(T_{ci} - e_s)\} / [\gamma (r_{awi} + r_{ci})], \tag{4}$$

where $e_s(T_{ci})-e_i$: difference between saturation vapor concentration at plant temperature and actual vapor concentration (m^3 m^{-3}),

r_{awi}: aerodynamic resistance for water vapor transfer in the ith layer (s m^{-1}),

r_{ci}: crop resistance in the ith layer (s m^{-1}).

After calculation of the sensible and latent heat, the estimation of the air temperature (T_{ai}) and vapor pressure (e_i) in the ith layer were as follows (*Goudriaan,* 1977):

$$T_{a,i} = T_{a,i-1} + H_i R_i / \rho c_p, \tag{5}$$

$$e_i = e_{i-1} + \lambda E_i R_i (\rho c_p / \gamma), \tag{6}$$

where R_i is a value characteristic to resistance in the ith layer (s m^{-1}). When $i=1$, $T_{a,i-1}$ and e_{i-1} are the temperature and water vapor pressure from the separated standard meteorological measurement, respectively.

The inputs of the model are site and plant specific parameters (plant height, leaf density in three layers), different soil characteristics (soil moisture content and physical properties) and hourly meteorological data are from standard measurements (*Goudriaan*, 1977). From the outputs the air temperature and humidity in the upper third of plant height are included in the study.

The meteorological data were provided by the local standard QLC automatic weather station.

The reconstruction of the Goudriaan model was designed to make the input of measured data easier and to display the results in a user-friendly manner. A further aim was to increase the maximum number of input data,

which was previously limited to 20. Nevertheless, the program still uses the basic equations elaborated by *Goudriaan* (1977).

To validate the model, the root mean square deviation (*RMSD*) of a number (*n*) of pairs of simulated (*S*) and measured (*M*) microclimate elements was applied:

$$RMSD = \left\{\left[\Sigma(M-S)^2\right]/n\right\}^{0.5} \tag{7}$$

The *RMSD* is one of the best overall measures of model performance (*Willmott,* 1982; *Castrignano et al.*, 1997).

The ear dry matter as a season long integrator of actual weather was measured at the end of the vegetation period by drying the samples to constant weight at 60 °C.

3. Results

3.1 Climatic conditions

The vegetation period in 2001 was substantially drier than the average, having 28.2% less rainfall than the many years' mean. If the monthly means are considered, the deviation from the 30-year mean was positive only in September, but in this case the difference was very great, since there was about 80 mm more rainfall than usual (*Fig. 1*).

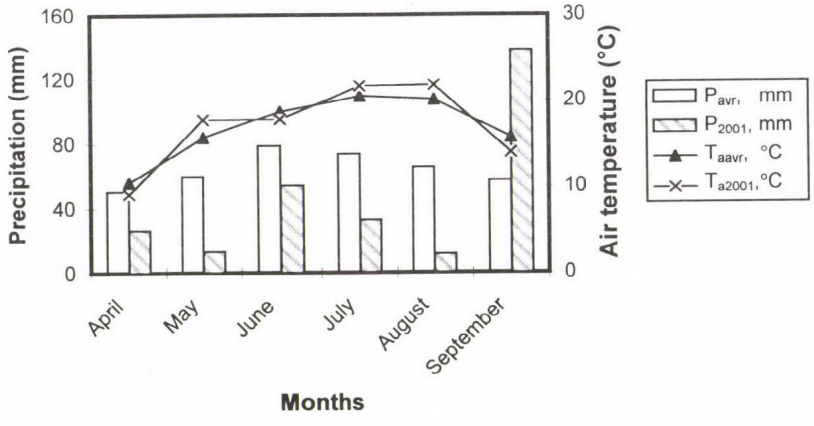

Fig. 1. Monthly precipitation sums and average air temperatures for 1970–1999 (P_{avr}, T_{aavr}) and in the season of 2001 (P_{2001}, T_{a2001}).

The water deficiency level for the vegetation period should thus be calculated without the September figures, in which case a value of 42.1% is

obtained. The distribution of the rainfall within the vegetation period may have caused a further deterioration in the growing conditions of maize, since the greatest deficiencies were observed in August, May, and July.

The rainfall deficiency during the periods when the water supply is critical for maize development was accompanied by warmer weather than usual. The mean monthly temperature was more than 2 °C higher in May and 1.2–1.7 °C higher in July and August than the normal values.

3.2 Size and distribution of the assimilatory surface

Irrigation increased the annual mean value of the green leaf area by 38.8%, mainly due to the delay in leaf withering in the irrigated stand (*Fig. 2*). The supplementary water supplies did not modify the date by which the greatest leaf area developed, but in the control treatment the extreme drought caused the lower leaf levels to wither by mid-August, so that practically the whole stand had become defoliated by the end of August. In the irrigated stand this did not occur until much later, in mid-September.

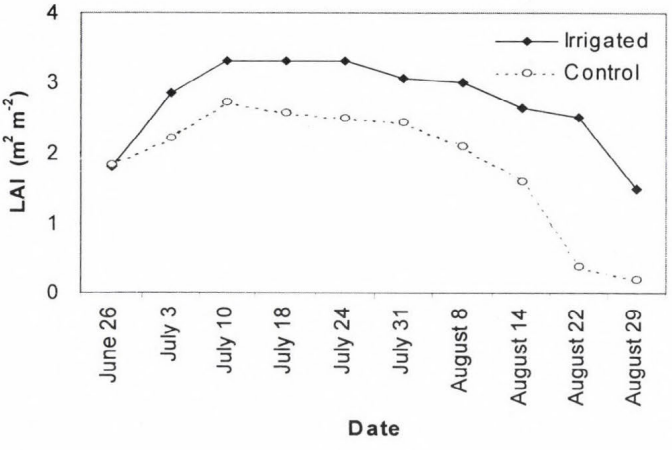

Fig. 2. Yearly trend in the leaf area index (LAI) of maize at two watering levels.

During the simulation, irrigation had a different effect on the leaf area distribution of the three plant height levels used as input parameters for the model. The three levels were obtained by simply dividing the total plant height by three (i=1,2,3). In the upper (i=1) and middle thirds (i=2) irrigation caused a constant increase in the leaf area (around 20% and 10% for the upper and middle thirds, respectively), while in the lower third, closest to the ground, due to the different extents of leaf withering, 14.2% deviation in leaf

area was recorded on July 10 as the result of irrigation, which was increased to 567.9% by the end of the month. The distribution of the total leaf area between the three levels during the simulation is presented in *Table 1* as a ratio of the leaf area of the upper third (the input parameter required by the model). Results in leaf area distribution of irrigated stand showed the success of irrigation during the 2001 season.

Table 1. Distribution of the leaf area over the different plant height levels as the ratio of the leaf area of the upper third (the input of the model)

	July 10	July 17	July 24	July 31	August 8
Irrigated plants					
Upper third	1	1	1	1	1
Middle third	1.56	1.56	1.56	1.56	1.56
Lower third	0.81	0.76	0.74	0.61	0.50
Control treatment					
Upper third	1	1	1	1	1
Middle third	1.73	1.73	1.73	1.73	1.73
Lower third	0.84	0.69	0.51	0.12	0.05

3.3 Irrigation and changes in CWSI

The water stress index is a complex index which provides a numerical indication of plant water deficiency, based on trends in plant properties and meteorological elements, before visible symptoms appear. During the 2001 vegetation period, the plants exhibited signs of water deficiency on four occasions due to the extreme drought (*Fig. 3*). The total water quantity in 2001, together with irrigation water, was 20 mm less than the long-term rainfall average for the vegetation period in the Keszthely region, suggesting that the irrigation was carried out very circumspectly (*Table 2*).

When the measurements began, double of the normal irrigation water amount was applied, since the mean water deficiency had already exceeded 70–80 mm. The *CWSI* is not suitable for the determination of earlier irrigation dates due to the nature of the plant temperature measurements which form the basis of the index. Plant temperatures characteristic of the stand can only be measured after canopy closure ($LAI \approx 2.0$–2.5 m^2 m^{-2}). This stage was reached at the end of June in 2001. (A greater quantity of water was also applied at the

last irrigation on August 8, since no further *CWSI* measurements or irrigation were planned.)

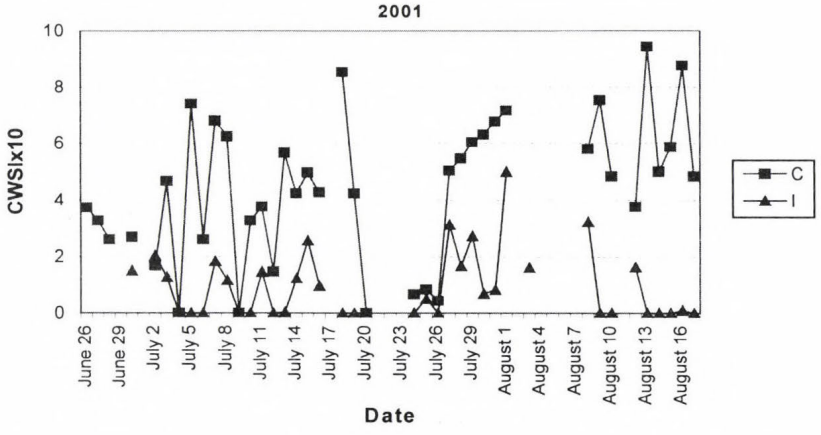

Fig. 3. Seasonal variation in crop water stress index of non-irrigated (C) and irrigated (I) plants. On cloudy days there were no samples taken, causing discontinuity in the figure.

Table 2. Quantity of irrigation water applied on each occasion in 2001

Irrigation date	Water rate (mm)	Intensity (mm/h)
June 28	60	6–8
July 15	35	6–8
August 1	18	6
August 8	56	6–8
Total	**169**	

Many papers have dealt with the difficulties of detecting plant temperatures, especially in semi-dry areas (*Keener* and *Kirchner,* 1983; *Jensen et al.* 1990; *Wanjura* and *Upchurch,* 1997). The greatest problem is caused by the disturbing effect of clouds on the intensity of the radiation and on the stand temperature; in some cases this may make the measurements impossible. This explains the lack of data in several places in *Fig. 3*, which depicts changes in *CWSI*. This often, but not always, coincided with the appearance of rainfall.

In 2001, a total of 170 mm of irrigation water was required to keep the *CWSI* value below the critical level and avoid damage to the life processes of the crop. Averaged over the whole measurement period, this water rate was sufficient to reduce the stress index by 131.6%. During the modeling period,

this change was somewhat more moderate, being only 116.9%. Irrigation led to a significant 22.4% rise in the grain yield (*Table 3*).

Table 3. Effect of irrigation on grain yields

	Irrigated treatment	**Control plants**
Yield (kg m^{-2})	0.80	0.68
Deviation	0.09	0.052
f test		0.598
t test		0.023
$LSD_{5\%}$		0.10

3.4 Microclimate simulation

3.4.1 Modification of the CMSM model (*Goudriaan*, 1977; *Goudriaan* and *van Laar*, 1994)

The program written by *Chen* in 1984 in BASIC programming language was unsuitable for automatic data input. Converting the input data before the program run was very time-consuming. The version elaborated by the authors is able to treat all the input data as parameters, thus reducing the running time considerably. In the original program the number of input data was limited to 20, but this has been expanded, since hourly measurements will mean at least twenty-four data a day. The new version of the program is also capable of displaying graphs, in addition to an hourly presentation of the data and the profiles of the elements (*Anda* and *Lőke*, 2002).

3.4.2 Results of the simulation

A microclimate simulation was carried out on the fully developed stand between the end of June and the beginning of August, 2001. The simulation was not a complete success on all the 38 days included in the study. On some of the sampling days, for reasons of extreme weather, the model either failed to run or the simulated values were substantially different from the measured values. On wet and windy days the deviation, especially for air humidity content, was more than 15–20% in all cases, the most extreme difference was 35%. For this reason, seven extremely stormy days – where the wind speed at 2 m above the canopy exceeded the 4–5 m s^{-1} and the amount of precipitation was above 5 mm – were excluded from the evaluation. The number of stormy day in 2001 was less than in most of the years.

In contrast to expectations, the presence of these meteorological elements, especially of wind, was less of a problem for the simulation of air temperature. The model could be run most successfully on bright, clear days. On some sample days, the simulation deteriorated substantially for some hours during the night, compared with the period from sunrise to sunset. The probably reason might has been the extreme weather of these days. In some cases, these data caused a substantial deterioration in the mean for the whole day. In order to avoid excluding further days from the evaluation, the success of the simulation was only calculated for the sunshine hours. This improved the estimation of the air temperature by a few tenths of a degree Celsius and that of relative humidity by around 5%. The results for sunshine hours were applied in further plant investigations such as stomatal resistance and photosynthesis (not published).

The justification for this procedure was that the change in the microclimate induced by the irrigation was relatively small in absolute terms, so even a deterioration of a few percent in the accuracy of the estimation may make the applicability of the method questionable. The sign of the deviation between the microclimate elements measured and calculated for the night hours was not the same on all of the days, though the values of relative humidity tended to be overestimated (*Fig. 4a, b*), and those of air temperature tended to be underestimated.

Irrespective of the water supplies, the most accurate microclimate simulation was obtained on clear days during the period from sunrise to sunset. The results are illustrated on the simulated and measured microclimate data of 5 irrigated and 5 control sample days. Averaged over the whole measuring period, the simulated air temperature mean for the sunshine hours was 0.27 °C higher than the true value in the control and 1.03 °C higher in the irrigated stand. (During the observation period, the greatest deviation found for the daylight hours was 1.07 °C in the control and 3.85 °C in the irrigated treatment.) The difference in the measured and simulated data for the mean air humidity during the daylight hours was 6.31% in the non-irrigated and 5.88% in the irrigated treatment. (The greatest deviation observed in the mean for the daylight hours was 13.94% without irrigation and 11.93% in the irrigated variant.) We compared measured and simulated data for the upper third of plant height.

On the basis of publication of *Pearcy et al.* (1991) on accuracy of estimation of the air temperature and humidity, the alteration between the measured and simulated microclimate elements is acceptable. The desirable accuracy of temperature measurements in plant studies is ± 1 °C. The wanted accuracy of relative humidity determination is about 20%.

(a) Non-irrigated control

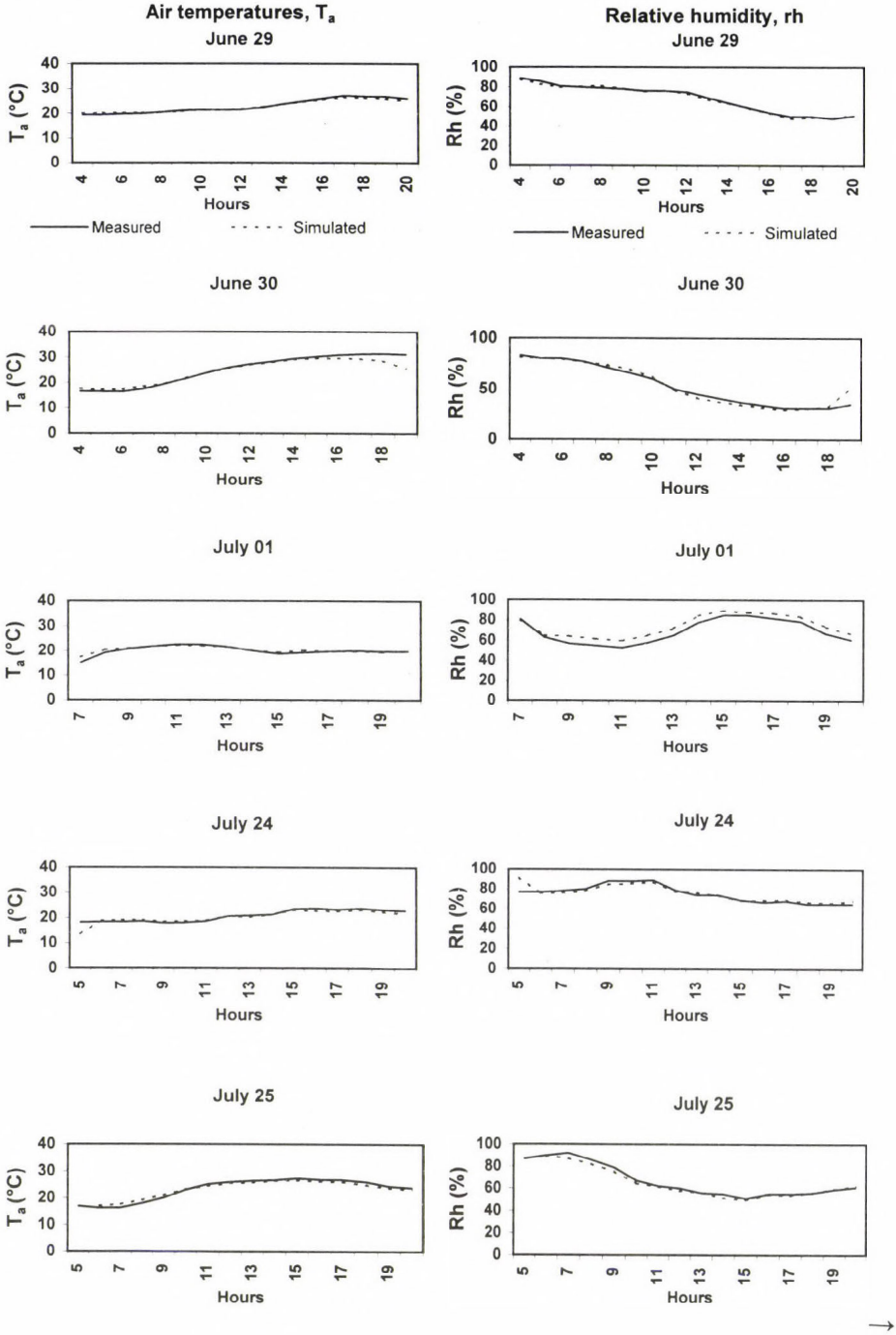

(b) Irrigated treatment

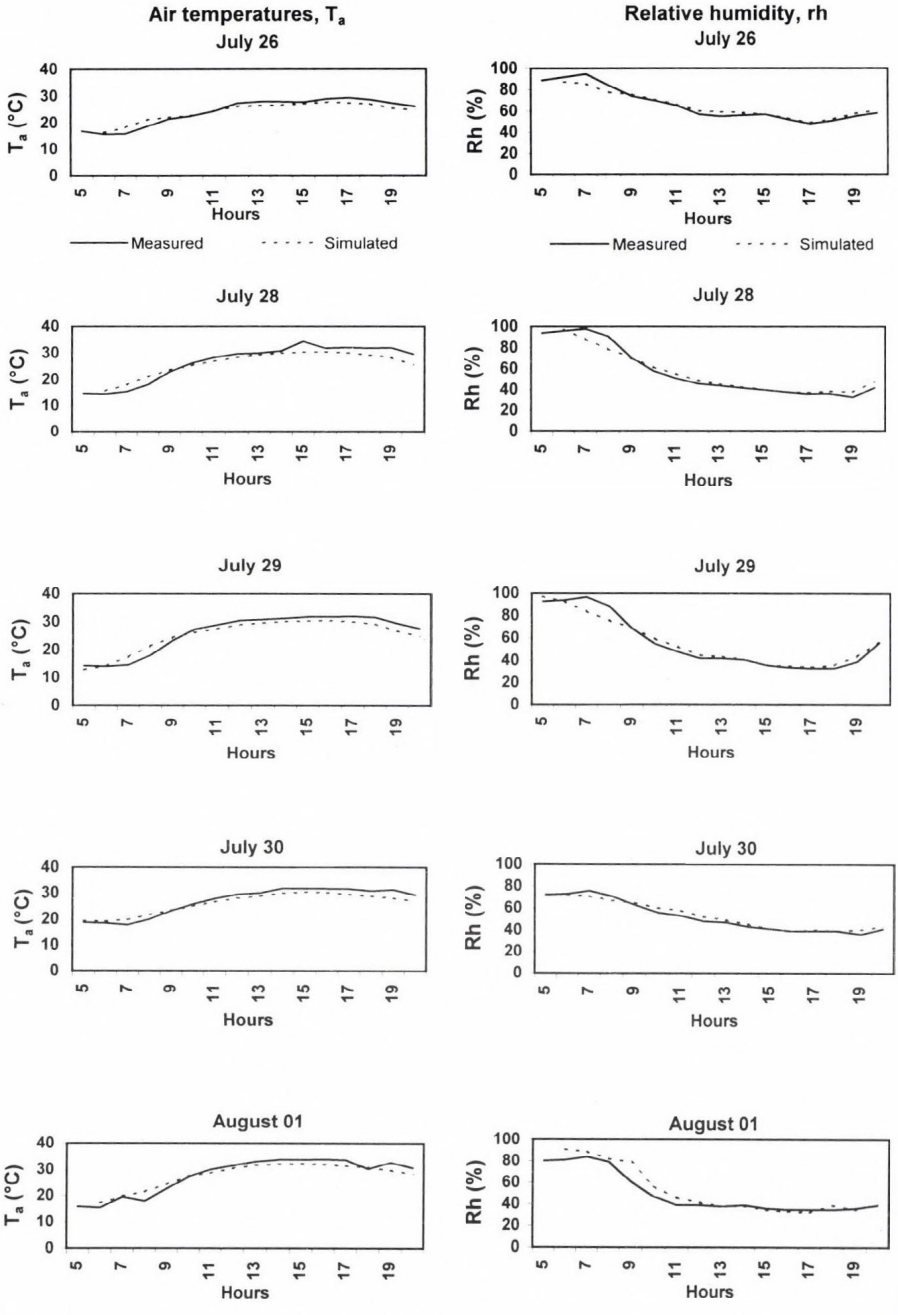

Fig. 4. Measured and simulated air temperatures and humidity in the upper third of plant stand on five sample days during 2001 in control (*a*) and irrigated (*b*) treatments, respectively.

3.5 Validation of the model

In the linear regression between simulated (P) and observed (O) values, $P = a + bO$, the intercept a was not significantly different from zero at $p = 0.05\%$, so a regression through the origin was applied. The slopes were close and not significantly different from 1. (Each 95% confidence interval includes 1, as *Table 4* shows.) We can conclude that the model well estimated both the air temperatures and relative humidity.

Table 4. Table of results in statistical analysis of measured and simulated data in the upper third of plant height

	Non irrigated control		**Irrigated treatment**	
	T_a	**Rh**	**T_a**	**Rh**
RMSD	0.474	3.055	0.931	2.780
Slope	0.997	1.003	1.013	0.961
95% confidence interval	[0.968;1.026]	[0.939;1.066]	[0.967;1.059]	[0.919;1.003]
R^2	0.999	0.998	0.999	0.999
Slope standard error	0.010	0.023	0.016	0.015
Regression root mean square error	0.525	3.408	0.966	1.913

4. Conclusions

Hourly values of the air temperature and humidity in the upper third of plant stand were simulated using the CMSM (*Goudriaan*, 1977; *Goudriaan* and *van Laar*, 1994) in irrigated and non-irrigated maize stands. Results in simulation were controlled by direct measurements after canopy closure during the 2001 growing season. The term of canopy temperature used in irrigation timing (*CWSI*) limited the beginning of the study (June 29–August 6). The aim of the investigation was to control the more precise and quick results on plant microclimate than that of we had earlier. The simulated elements of microclimate could serve a good basis in plant studies, because almost all physiological processes deeply depend on those parameters surround the plants.

- Among the microclimate elements, the accuracy of the estimation of air temperature in the upper third of non-irrigated stands was better than that found for irrigated stands. In the case of humidity, the deviations between the simulated and measured elements were similar for the two water supply treatments. In order to reduce the difference, the estimations for the night hours were ignored, since the error of these values was greater than that of the simulation for the daylight hours. Using this technique, the accuracy of estimation for the investigated parameters improved, since the differences in air temperature values dropped to 0.5–1.0 °C and those of air humidity dropped below 10%. These deviations were small enough to enable the slight changes caused by irrigation to be detected. The limited use for sunshine hours is acceptable when plant physiological processes are studied, but further investigations are needed.

- Provided, that the distribution of the leaf area between the various levels of the plant stand is known, the *Goudriaan* (1977) model appears to be suitable for the demonstration of changes in the microclimate as the result of irrigation, even if these are very slight. This could be of importance in predicting the probable effect of human interventions. In particular, a new light could be shed on the relationship between the changes in air humidity and the multiplication of certain plant diseases, which could lead to more efficient planning of disease control measures.

- At present the model is the most satisfactory for the simulation of the daylight hours of clear days. When the wind speed exceeded 4–5 m s^{-1} above the stand and the amount of precipitation was above 5 mm, the accuracy of simulation deteriorated (seven days from 38). Further research will be required to make it adaptable for rainy, windy days.

Acknowledgement—The study was sponsored by the Hungarian Academy of Sciences under the work of T 043147.

References

Anda, A., 1993: The use of infrared thermometry in irrigation timing (in Hungarian). *PhD Thesis*. MTA, Budapest.

Anda, A. and *Stephens, W.*, 1996: Sugar beet production as influenced by row orientation. *Agron. J. 88*, 991-996.

Anda, A. and *Lőke, Zs.*, 2002. Modelling the factors determining maize evapotranspirotaion: The stomatal resistance, surface temperature and photosynthesis (in Hungarian). *Növénytermelés 52*, 351-363.

Anda, A., Lőke, Zs., and *Burucs, Z.*, 2001: Microclimate of irrigated and non-irrigated maize (in Hungarian). *Növénytermelés 50*, 249-260.

Calveta, J.C., 2000: Investigating soil and atmospheric plant water stress using physiological and micrometeorological data. *Agr. Forest Meteorol. 103*, 229-247.

Calveta, J C., Noilhana, J., Roujeana, J.L., Bessemoulina, P., Cabelguenneb, M., Oliosoc, A., and *Wigneroc, J.P.*, 1998: An interactive vegetation SVAT model tested against data from six contrasting sites. *Agr. Forest Meteorol. 92*, 73-95.

Carberry, P.S., Muchow, R.C., and *McCown, R.L.*, 1989: Testing the CERES-Maize simulation model in a semi-arid tropical environment. *Field Crop. Res. 20*, 297-315.

Castrignano, A., Di Bari, V., and *Stelluti, M.*, 1997: Evapotranspiration predictions of CERES-Sorghum model in Southern Italy. *Eur. J. Agron. 6*, 265-274.

Cavero, J., Playán, E., Zapata, E., and *Faci, M.J.*, 2001: Simulation of maize grain yield variability within a surface-irrigated field. *Agron. J. 93*, 773-782.

Chen, J., 1984: Mathematical analysis and simulation of crop micrometeorology. *Ph.D. Thesis*. The Netherlands.

Evans, G.C., 1972: *The Quantitative Analysis of Plant Growth*. Blackwells, Oxford.

Fodor, N., Mathene-Gaspar, G., Pokovai, K., and *Kovacs, G.J.*, 2003: 4M-software package for modelling cropping systems. *Eur. J. Agron. 18*, 389-393.

Franks, S.W., Beven, K.J., Quinn, P.F., and *Wright, I.R.*, 1997: On the sensitivity of soil-vegetation-atmosphere-transfer (SVAT) schemes: Equifinality and the problem of robust calibration. *Agr. Forest Meteorol.* 86, 63-75.

Gardner, B.R., Blad, B.L., and *Watts, D.G.*, 1981: Plant and air temperatures in differentially irrigated corn. *Agr. Meteorol. 25*, 207-217.

Gottschalk, J.C., Gillies, R.R., and *Carlson, T.N.*, 2001: The simulation of canopy transpiration under doubled CO_2: The evidence and impact of feed-backs on transpiration in two 1-D soil-vegetation-atmosphere-transfer models. *Agr. Forest Meteorol. 106*, 1-21.

Goudriaan, J., 1977: *Crop Micrometeorology: A Simulation Study*. Simulation monographs. Pudoc, Wageningen.

Goudriaan, J. and *van Laar, H.H*, 1994. *Modelling Potential Crop Growth Processes*. Kluwer Academic Publishers, Dordrecht-Boston-London. 238p.

Hatfield, J.L., 1990: Measuring plant stress with an infrared thermometer. *Hort. Science 25*, 1535-1538.

Huzsvay, L. and *Nagy, J.*, 1994: An analysis on correlation between plant number and yield in maize by models with different biological validity (in Hungarian). *Növénytermelés 43*, 533-544.

Idso, S.B., Jackson, R.D., Pinter, P.J. Jr, Reginato, J.R., and *Hatfield, J.L.*, 1981: Normalising the stress degree parameter for environmental variability. *Agr. Meteorol. 24*, 45-55.

Irmak, S., Haman, D.Z., and *Bastug, R.*, 2000: Determination of CWSI for irrigation timing and yield estimation of corn. *Agron. J. 92*, 1221-1227.

Jackson, R.D., 1982: Canopy temperature and Crop Water Stress. *Adv. Irrig. 1*, 43-85.

Jackson, R.D., Idso, S.B., Reginato, R.J., and *Pinter, P.J. Jr.*, 1981: Canopy temperature as a crop water stress indicator. *Water Resour. Res. 17*, 1133-1138.

Jensen, H.E., Svendsen, H., Jensen, S.E., and *Mogensen, V.O.*, 1990: Canopy-air temperature of crops grown under different irrigation regimes in a temperate humid climate. *Irrigation Sci. 11*, 181-188.

Jones, H.G., 1983: *Plants and Microclimate*. Cambridge Univ. Press, Cambridge. 323p.

Jones, C.A. and *Kiniry, J.Y.*, 1986: CERES-Maize: A simulation model of maize growth and development. Texas A&M Univ. Press, College Station.

Keener, M.E. and *Kirchner, P.L.*, 1983: The use of canopy temperature as an indicator of drought stress in humid regions. *Agr. Meteorol. 28*, 339-349.

Kiniry, J.R. and *Knievel, D.P.*, 1995: Response of maize seed number to solar radiation intercepted soon after anthesis. *Agron. J. 87*, 228-234.

Kiniry, J.R., and *Bockholt, A.J.*, 1998: Maize and sorghum simulation in diverse Texas environments. *Agron. J. 90*, 682-687.

Kiniry, J.R., Williams, J.R., Richard, L., Vanderlip, J.D., Atwood, D., Reicosky, C., Mulliken, J., Cox, W.J., Mascagni, H.J., Hollinger, S.E., and *Wiebold, W.J.*, 1997: Evaluation of two maize models for nine U.S. locations. *Agron. J. 89*, 421-426.

Liu, W.T.H., Botner, D.M., and *Sakamoto, C.M.,* 1989: Application of CERES-Maize to yield prediction of a Brazilian maize hybrid. *Agr. Forest Meteorol. 45,* 299-312.

Mantovani, E.C., Villalobos, F.J., Orgaz, J., and *Fereres, E.,* 1995: Modelling the effects of sprinkler irrigation uniformity on crop yield. *Agr. Water Manage. 27,* 243-257.

Nobel, P.S., 1974: *Introduction to Biophysical Plant Physiology.* Freeman Press, San Francisco.

Nouna, B.B., Katerji, N., and *Mastrorilli, M.,* 2001: Using the CERES-Maize model in a semi-arid Mediterranean environment. Evaluation of model performance. *Eur. J. Agron. 13,* 309-322.

Paz, J.O, Batchelor, T.S., Colvin, S.D., Logsdon, T.C., Kaspar, C., and *Karlen, D.L.,* 1998: Analysis of water stress causing spatial yield variability in soybeans. *Trans. ASAE, 41,* 1527-1534.

Pearcy, R.W., Ehleringer, J., Mooney, H.A., and *Rundel, P.W.,* 1991: *Plant Physiological Ecology.* Chapman and Hall, London-New York-Tokyo, 457p.

Plantureaux, S., Girardin, P., Fouquet, D., and *Chapot, J.Y.,* 1991: Evaluation et analyse de sensibilité du modéle CERES-Maize en conditions alsaciennes. *Agronomie 11,* 1-18.

Rosenberg, N.J., 1974: *Microclimate: The Biological Environment.* Wiley, New York.

Sellers, W.D., 1965: *Physical Climatology.* Chicago, Univ. of Chicago Press.

Stockle, C.O. and *Kiniry, J.R.,* 1990: Variability in crop radiation use efficiency associated with vapor pressure deficit. *Field Crop. Res. 21,* 171-181.

Wanjura, F. and *Upchurch, D.R.,* 1997: Accounting for humidity in canopy-temperature-controled irrigation scheduling. *Agr. Water Manage. 34,* 217-231.

Willmott, C.J., 1982: Some comments on the evaluation of model performance. *B. Am. Meteorol. Soc.,* 1309-1313.

de Wit, C.T. and *Goudriaan, J.,* 1978: *Simulation of Ecological Processes.* Wageningen, Pudoc.

Xie, Y., Kiniry, J.R., Nedbalek, V., and *Rosenthal, W.D.,* 2001: Maize and sorghum simulations with CERES-Maize, SORKAM, and ALMANAC under water limiting conditions. *Agron. J. 93,* 1148-1155.

IDŐJÁRÁS

Quarterly Journal of the Hungarian Meteorological Service
Vol. 109, No. 1, January–March 2005, pp. 39–53

On the use of standard meteorological data for microclimate simulation

Márta Hunkár

Department of Mathematics, Georgikon Faculty of Agriculture, University of Veszprém
P.O. Box 71, H-8360 Keszthely, Hungary; E-mail: hunkar@georgikon.hu

(Manuscript received in final form January 19, 2005)

Abstract—Multi-layer microclimate simulation models describe the profiles of meteorological variables inside the canopy. For a steady state model, the instantaneous values of air temperature, vapor pressure, wind speed, and global radiation are needed as input variables from a given height above the canopy. A standard automatic meteorological station provides all those data with high frequency in time, but from outside of the canopy. A simple calculation method is presented in this paper for evaluation „above canopy" data from standard data. Roughness parameters are considered in three different ways. Applying the methods for an experimental maize field, measured plant characteristics were used. At the beginning of the vegetation season and in the senescence period, the differences in roughness parameters due to different approaches were negligible, the largest difference in roughess parameters occured at the fully developed plant stand. The differences occurred due to application of the calculated different roughness parameters in profiles of meteorological elements were small even at this time. We concluded that data transferring is needed because of keeping consistency among meteorological data, at least plant height must be taken into account in determination of surface roughness length and zero-plane displacement. Further plant characteristics as LAI, the width of the leaves, and the drag coefficient of the leaves can also be taken into account, for it makes the method more general, but in the case of maize stand, the effect on the profiles of meteorological elements is rather small.

Key-words: microclimate, surface roughness length, zero-plane displacement, simulation model

1. Introduction

The processes of energy exchange and flow of materials between the surface and the atmosphere provide all the conditions which are important for crop growth and also for parameterization of General Circulation Models. Taking a

vegetated surface, a soil vegetation atmosphere transfer scheme (SVAT) describes the fluxes of heat, water vapor, and CO_2 between a multi-component vegetated land surface and the atmosphere. The SVAT models are different in their complexity. The SVAT "big-leaf" models treats the canopy and underlying substrate as a single source (*Ács*, 1994). In a two-source model, the canopy component is treated either as a single big leaf, or as partitioned shaded-sunlit leaves (*Sellers et al.*, 1996; *Tourula et al.*, 1998; *Boegh et al.*, 1999). Transports of heat and soil moisture are often represented with three or more layers (*Flerchinger et al.*, 1998). The number of layers mostly depends on the purpose of the SVAT model. In land-surface hydrology, the soil is divided into several layers and vegetation is presented by one layer (*Ács* and *Hantel*, 1998, 1999; *Ács* and *Kovács*, 2001).

In production ecology, the basic question is how internal and external factors influence the growth and development of crops. Micrometeorological conditions within a crop canopy are important as direct environmental forces to photosynthesis, and also for the microorganisms living in the ecosystem. Therefore, a multi-layer approach for the vegetation is important to describe vertical profiles of air temperature, humidity, wind speed as micrometeorological conditions within the plant canopy. Those profiles depend on macrometeorological conditions prevailing above the canopy, and the structure and water status of the soil and the plant stand.

Information about meteorological conditions inside the canopy is often needed because of any kind of practical purpose, but direct measurement of the elements with a special mast equipped with sensors are not available inside and above the canopy. Meteorological stations are installed outside of the plant stand, concerning WMO standards: temperature and air humidity are measured at 2 m height in shelter, wind speed at 10 m height in open area, incoming global radiation at an open area. Nevertheless, the automation of the measurements provides meteorological data with high frequency in time, the problem is the place of the measurements. If we want to use micrometeorological model, we need data from a reference height above the canopy. For operational purpose, a rather crude solution might be that measured values of meteorological elements are taken directly as model inputs with fixed height of reference level. Statistical data analysis carried out by *Anda et al.* (2003) did not find significant differences between the data measured at the standard meteorological station and above the canopy, for the experimental site at Keszthely Agrometeorological Research Station. Nevertheless, in micrometeorology, "differences" are small and vary also in plus-minus direction in time for day-time and night-time, therefore, statistical relations are not applicable to get instantaneous values of the meteorological elements. A further viewpoint is keeping the physical consistency of data.

In this paper a simple solution is given to overbridge this problem for the situation of Keszthely Agrometeorological Station and experimental field. Nevertheless, the method is applicable for other places as well where the meteorological station is close enough to the field. It has to be emphasized, that our main purpose is to make an existing micrometeorological model to be operative by providing the required initial values.

2. Crop Micrometeorological Simulation Model

Crop Micrometeorological Simulation Model, CMSM, developed by *Chen* (1984a) gives detailed calculations of the profiles of meteorological elements within a plant stand. The basic equations of the model are summarized by *Goudriaan* (1977). The model consists of three main parts: radiation submodel which gives results both on macroscale (crop reflectance and transmittance) and microscale (distribution of absorbed radiation intensity over the leaves); the energy and mass balances of leaves and soil surface, which connects the radiation model to the phenomena of transpiration and photosynthesis; aerodynamical submodel for wind and turbulence, which are treated as related phenomena above as well as inside the canopy. CMSM is a multi-layer steady state model, according to the air conditions, assuming equilibrium at any time in the air, and dynamic for the soil heat transfer because of the significant value of soil heat capacity. Momentum-, sensible heat-, and latent heat transfer are calculated between the soil surface and the bottom layer, and between the individual layers of the canopy, as well as between the top of the canopy and the reference height. The fluxes are controlled by radiative forcing and aerodynamical resistances. A detailed description of fluxes and numerical solutions are given by *Chen* (1984b). Instability is considered by the Monin-Obukhov length, L, which has to be given as initial value for the time zero, but it is only a „first guess", the model calculates its actual value for each time step. The time step of the model is optional, it is worth to choose few minutes. In our simulation experiments, 10 minutes were chosen for time step. Using that flux values, the actual air- and leaf temperature and vapor pressure are calculated "backward". In real world, differences in temperatures and vapor pressure between the surface and the surrounding air, and between the individual layers generate fluxes of sensible and latent heat, and the values of meteorological elements above the canopy are controlled and determined by the energy exhange taking place at the leaves and soil, transferring by the fluxes on dynamic way. According to the CMSM concept, we know the results of these processes, namely the actual values of air temperature and vapor pressure at the reference height above the canopy at any time, therefore, the

fluxes resulting them can be calculated as well as the temperature and vapor pressure gradient.

It means that input meteorological data required by CMSM derive from measured data at a reference height above the canopy, those are: instantaneous values of global radiation, air temperature, vapor pressure, wind speed at any time characterizing daily course of the elements. Linear interpolation is used to get those values for the individual time steps. Soil heat transfer is calculated on dynamic way, therefore, the initial values of soil temperature profile must be given at time zero (usually at midnight).

The model was tested in Hungary as well, using measured meteorological, soil and plant data (*Hunkár*, 1990). Later on a user-friendly version was developed (*Hunkár*, 2002), which makes easier data handling and output interpretation on WINDOWS basis.

3. Description of the measurements and adjusments

At the site of the Agrometeorological Research Station at Keszthely (46°46'N; 17°20'E) an automatic meteorological station runs according to WMO standards. The place for meteorological measurements is located near the experimental field of maize, where micrometeorological characterization is required. Air temperature and humidity sensors are in a shelter located about 20 m from the edge of the maize field at 2 m height above the ground surface. Wind sensor is located at the top of a mast of 10 m height, and global radiation is also measured at the same mast at 5 m height. The mast is settled at the edge of the maize field. The ground surface below the station is covered with short grass. To have daily course of the elements, ten minutes average values between the 50th–60th minutes in each hour will be used from 00:00 until 24:00 CET.

There are different ways to get the required meteorological data above the canopy. One possibility is that the reference height is fixed at given height above the ground surface, and we have to modify the measured data, taking into account the theorethical shape of the vertical profiles of the elements, considering the surface roughness length, zero-plane displacement, and thermal stability. Another possibility is to choose a reference height where the data would be the same as the measured value. The values of surface roughness length and zero-plane displacement are also used for this approach. Both ways shall be used to get appropriate meteorological data (*Fig. 1*). In the case of air temperature and vapor pressure, we use the values measured at the meteorological station searching for the level above the canopy, where the same values could be occurred. Thermal stratification is assumed to be the

same both outside and above the canopy, therefore, the height of the reference level is different from the level of "outside" measurements just because of the roughness length and zero-plane displacement characteristic for the plant stand. In the case of wind, the measured data – which came from 10 m height – will be transformed to that reference level using logarithmic wind profile.

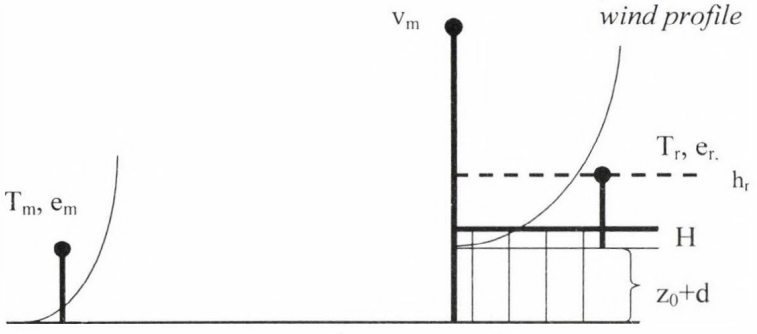

Fig. 1. The concept of data transformation. T_m, e_m are the measured values of air temperature and vapor pressure outside of the canopy at 2 m height, v_m is the measured wind speed at the edge of the canopy at 10 m height, T_r, e_r, v_r are those values transformed to the reference height, h_r is the reference height above the canopy, z_0 is the roughness length, d is the zero plane displacement, H is the height of the canopy (after *Szász* and *Tőkei*, 1997).

Horizontal advection is not taken into account, therefore, the method is applicable only when the place of meteorological measurement is close to the plant stand.

3.1 Surface roughness length and zero-plane displacement

The crucial point in our method is assessing a proper value of surface roughness length, z_0, and zero-plane displacement, d. A sensitivity study carried out by *Weidinger et al.* (2000) showes the strong dependence of sensible heat flux on surface roughness length and zero-plane displacement height. Most of the studies concerning the exchange of mass and energy between the surface and the atmosphere are based on wind profile observations. A high tower equipped with sensitive anemometers is rather expensive, therefore, only small set of actually measured roughness parameters are available. *Wieringa* (1993) analyzed and summarized about fifty well documented experiments over various surfaces. When the surface is covered

by vegetation, the roughness parameters are determined by the structure of the plant stand, which is changing in time as plant grows. *Monteith* (1973) suggested an empirical linear relation for d using measured value of plant height, H:

$$d=0.63H. \tag{1}$$

The length of z_0 is often supposed to be about one tenth of the height of the vegetation:

$$z_0=0.1H. \tag{2}$$

Tanner and *Pelton* (1960) suggested an empirical formula for surface roughness length, z_0:

$$\log_{10} z_0 = 0.997 \log_{10} H - 0.883. \tag{3}$$

Stanhill (1969) gives also an emprical formula for zero plane displacement, d:

$$\log_{10} d = 0.9793 \log_{10} H - 0.1536. \tag{4}$$

In Eqs. (1)–(4) the plant stand is characterized only with the height of the plants. Thinking on the roughness characteristics of a vegetated surface it is clear, that leaf area density and the drag coefficient of the leaves affect the strength of the sink for momentum, too. The greater the leaf area density belonging to the same plant height, the surface seems to be smoother with less z_0 but higher d, and, of course, a hairy type leaf makes stronger drag than a plain leaf.

A sophisticated and physically based calculation is used by *Goudriaan* (1977) which takes into account not only the height of the plant stand, H, but the leaf area index, LAI, the average width of the leaves, w, and the drag coefficient of the leaves, c. In our work the values of d and z_0 are considered after the theoretical description of *Goudriaan* (1977), which were applied in the model of *Chen* (1984a),

$$d = H - \sqrt{\frac{l_m \cdot a}{k}}, \tag{5}$$

where l_m is the mixing length, a is the extinction coefficient for wind inside the canopy, k is the Karman constant, 0.4. For the mean mixing length in the canopy the free space between the leaves or stems is used. The number of leaves per volume is given by $L_d w^{-2}$, where w is the width of the leaves and L_d is the leaf area density which comes from the measured values of leaf area index (LAI) and canopy height, H: $L_d=LAI/H$. When the leaves are long and

narrow, the mean mixing length is the diameter of a cylinder, containing on the average one leaf. Mixing length is calculated by

$$l_m = i_w \cdot \sqrt{\frac{4 \cdot w \cdot H}{\pi \cdot LAI}}, \tag{6}$$

where i_w is the relative turbulent intensity, a proportionality factor that expresses that eddy velocity or friction velocity is proportional to the local wind speed. After measurements of *Shaw et al.* (1974), the averege value for maize is taken as 0.5 as first approach.

The extinction coefficient for wind inside the canopy is calculated using plant characteristics as well:

$$a = \sqrt{\frac{c \cdot LAI \cdot H}{2 l_m}}, \tag{7}$$

where c is the drag coefficient of leaves, taken as 0.3.

Surface roughness length is determined by the formula:

$$z_0 = (H - d) \cdot \exp\left\{-\frac{H}{a \cdot (H - d)}\right\}. \tag{8}$$

Table 1. Roughness length and zero-plane displacement at different developmental stages of the maize stand* calculated after different authors (Keszthely, 1999 cv: Marietta)

Plant characteristics		**Height of the plants (m)**	**Roughness length (m)**			**Zero-plane displacement (m)**		
Leaf width (m)	**LAI (m^2m^{-2})**		***Monteith* (1973)**	***Tanner* and *Pelton* (1960)**	***Goudriaan* (1977)**	***Monteith* (1973)**	***Stanhill* (1969)**	***Goudriaan* (1977)**
0.02	0.5	0.5	0.05	0.065	0.071	0.315	0.356	0.263
0.04	1.75	1.0	0.1	0.130	0.089	0.630	0.702	0.750
0.05	2.5	1.5	0.15	0.196	0.100	0.945	1.044	1.224
0.05	3.5	2.0	0.2	0.261	0.099	1.260	1.384	1.729
0.05	3.8	2.5	0.25	0.326	0.103	1.575	1.722	2.214

* leaf width and LAI have also changed in the approach of Goudriaan, while other authors take only plant height

A comparison of the results of calculated values of d and z_0 is presented in *Table 1* for the maize stand. Plant characteristics as *LAI* and leaf width represent the average interpolated values belong to the given height. Surface

roughness length (z_0) increases with smaller rate with the plant height according to *Goudriaan* (1977) approches, but zero-plane displacement (d) has a greater rate with plant height, therefore, the aerodynamic depth of the plant stand became higher when plant height exceeds 1 m. For a full developed maize stand the difference in z_0+d is about 0.5 m according to the different methods (*Fig. 2*).

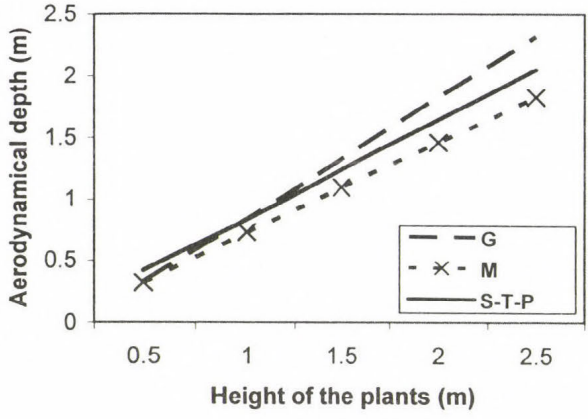

Fig. 2. Aerodynamical depth (z_0+d) of the plant canopy versus plant height according to the different approaches G: *Goudriaan* (1977), M: *Monteith* (1973), S-T-P: *Stanhill* (1969) and *Tanner* and *Pelton* (1960).

3.2 Vapor pressure and temperature

In the case of temperature and humidity, the measured data, T_m and e_m derive from 2 m height above the surface outside of the canopy. If we knew the depth of the aerodynamically active layer in the plant canopy, z_0+d, the data can be transferred adding that 2 m to the height of the active surface in the canopy (see *Fig. 1*). That height, the so called reference height, h_r, depends on the surface roughness length, z_0, and the zero-plane displacement, d. It is a significant simplification that thermal stratification, hereby the profiles of temperature and vapor pressure are assumed to be the same at the meteorological station and above the maize canopy, only the zero level is different. Roughness length for a surface covered by short-cut grass is not exceeds 0.01 m, it is neglected in calculation of the height of the reference level. Since the radiation regime and soil properties, as well as soil moisture content for a short-cut grass and maize at the same site are similar, the differences in the vertical temperature and vapor pressure gradient are not

taken into account. The error caused by this simplification is acceptable. The reference height,

$$h_r = z_0 + d + 2 \text{ meters}, \tag{9}$$

and the measured values of air temperature, T_m, and vapor pressure, e_m, at the meteorological station can be used as the air temperature, T_r, and vapor pressure, e_r, at the reference height above the canopy:

$$T_r = T_m \tag{10}$$

$$e_r = e_m. \tag{11}$$

As the characteristics of the plants change during the vegetation period, the height of reference level will also change in time. Since the height of the reference level is optional as an input data in the simulation model, it can and must be changed according to the development of the plant stand.

3.3 Wind speed at the reference height

Wind speed was measured at the top of a mast with 10 m height at the edge of the plant stand. Since the location of the mast was under the influence of the aerodynamical effects of the plant stand, in our case wind data were considered as "above canopy" data where roughness characteristics were taken from the plant stand. CMSM is a one-dimensional model having only vertical fluxes, wind data means only wind speed, wind direction is not considered, therefore, fetch distance is not considered as well. In other cases, when the place of wind measurement is an open area outside of the plant stand, the different drag characteristics of the different surfaces as well as wind direction have to be taken into account for calculation of fetch. At the experimental site of Keszthely measured wind speed data have to be transferred to the reference height determined before. The profile of wind velocity above the canopy can be represented by a logarithmic relation:

$$U = \frac{u^*}{k} \ln \frac{z-d}{z_0}, \tag{12}$$

$$u^* = k \cdot \frac{U}{\ln \frac{(z-d)}{z_0}}, \tag{13}$$

where U is the wind velocity at 10 m height, u^* is friction velocity, $z = 10$ m, k, d, and z_0 are as before. In this approach d and z_0 do not depend on the wind

speed, therefore, the relationship between u^* and U is linear, but some authors found nonlinear relationship explained by the assumption that z_0 and d are influenced by the wind speed (*Long et al.*, 1964; *Tajchman*, 1981). Others found this effect non significant (*Munroe* and *Oke*, 1973). Recently *Hurtalova* and *Matejka* (1999) analyzing profile measurements carried out within the framework of NOPEX CFE1 gave numerical relationship between the wind speed and roughness properties, z_0 and d. It is seems to be logic, that a strong wind makes the surface smoother when it is covered by flexible stalks of grasses or cereals. *Hurtalova et al.* (2004) analyzed wind profiles above maize canopy, and found nonlinear dependence of friction velocity on the wind speed. Nevertheless, when wind speed is moderate or week, the effect might be neglected. In our consideration this effect is not taken into account.

Having the value of u^* from Eq. (13), the wind velocity at the reference height, U_r is

$$U_r = \frac{u^*}{k} \ln \frac{h_r - d}{z_0}. \tag{14}$$

3.4 Global radiation

In the case of global radiation there is nothing to do, because the model uses the incoming radiation, and the distance of the measuring place from the plant canopy is so small, that there is no need to change the measured data of global radiation.

4. Model simulations

4.1 Data sets and parameters

During the vegetation season in 1999, the soil and plant characteristics were measured ten times from June 1 until September 1. Measured plant characteristics were determined using 10 sample plants each time. The height of the plants, the length of each leaves, and the maximum width of each leaves were measured with tape-measure. The average width of the leaves came from the maximum width multiplying by 0.75. The average values of soil water potential for upper one meter depth are shown in *Table 2*. Water potential of the soil was used in CMSM in determination of plant water status, which affects the stomatal resistances and, therefore, the latent heat flux. The values of soil water potential change between -0.1 bar at field capacity and -15 bar at wilting point for any type of soil. The changes in the height of reference level during the vegetation season in 1999 are presented in *Fig. 3*, as it was calculated by different approaches.

Table 2. Plant and soil characteristics used by the crop micrometeorological model. (The line with grey background shows the experiment analyzed in details.)

Date	Height of the crop (m)	Leaf area index ($m^2\ m^{-2}$)	Average width of the leaves (m)	Average soil water potential for 1 m depth (bar)
June 1	0.48	0.48	0.02	–0.96
June 11	0.58	0.75	0.03	–1.20
June 21	0.7	1.33	0.04	–0.88
July 1	1.5	2.49	0.05	–1.28
July 13	2.1	3.52	0.05	–0.80
July 20	2.2	3.56	0.05	–1.26
August 3	2.2	3.48	0.05	–2.20
August 12	2.2	3.24	0.05	–3.80
August 23	2.2	2.58	0.05	–3.35
September 1	2.2	1.95	0.05	–2.65

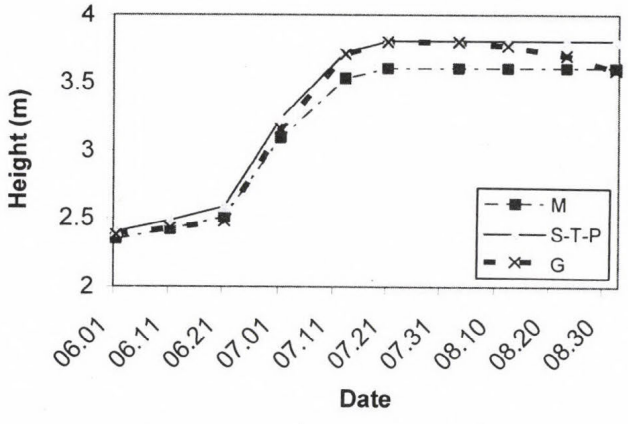

Fig. 3. Height of the reference level during the vegetation season, z_0+d is determined by different approaches G: *Goudriaan* (1977), M: *Monteith* (1973), S-T-P: *Stanhill* (1969) and *Tanner* and *Pelton* (1960).

The largest difference caused by the different methods occurs at the fully developed plant stand, it is about 0.2 m. This difference may cause some change in the calculated wind speed data, which is one of the required inputs

for the model. In *Fig. 4* measured and calculated wind speed data are shown for July 20, according to determination of z_0 and d suggested by *Monteith* (1973) and *Goudriaan* (1977), respectively. Some difference occur only around noon and they do not exceed 0.02 m s^{-1}. Since in other time the differences in reference height is even less the model outputs are shown only for this time.

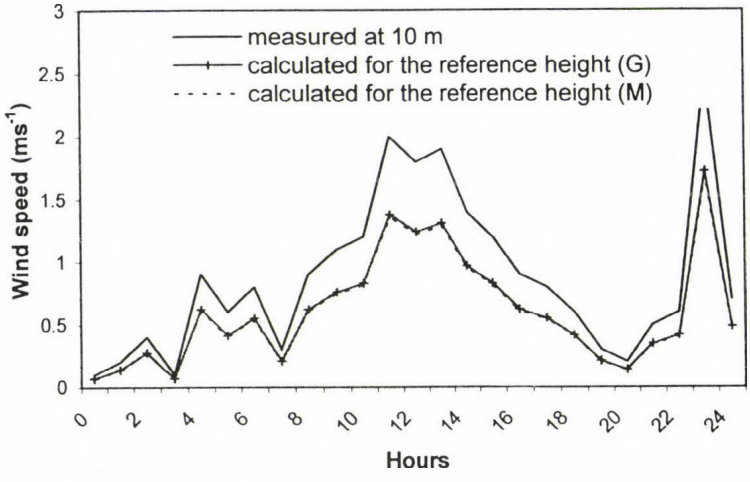

Fig. 4. Wind speed on July 20, 1999, measured at 10 m height, and calculated for different reference levels; M: h_r=3.6 m, G: h_r=3.8 m.

The CMSM is a multi-layer model. The canopy was divided into three layers, all of them have the same leaf area index, therefore, the depth of the layers are changing with the development of the plants. Vertical profiles of leaf area are given in the parameter sets that can be measured experimentally or calculated hypothetically. For a fully developed maize stand, parabolic *LAI* profile can be assumed, but at the beginning of the growing season and in the scenescence period the leaf area has different shape. The depth of the layers for the simulation experiment on July 20, 1999 was determined experimentally that LAI=3.56 was divided by 3, so each layer has LAI_i=1.19 (i=1,2,3), and the depth of the layers are as follows: 0.85 m, 0.66 m, and 0.69 m from the bottom to the top of the canopy.

4.2 Scenarios for simulations

To compare the model outputs, the model was run with different reference heights calculated by different methods of calculation of roughness length and

zero-plane displacement. We show the differences in the profiles of meteorological elements inside and above the canopy calculated by the model only to that time, when the largest difference occurred in the reference height, i.e., on July 20, 1999, at 12:00 CET (*Fig. 5*). Scenario M means that z_0 and d were determined after *Monteith's* (1973) suggestion, scenario G means the method of *Goudriaan* (1977). Since the logarithmic formula suggested by *Stanhill* (1969) and *Tanner* and *Pelton* (1960) resulted in the same values of z_0 and d as Goudriaan's one for that time (see in *Fig. 3*), we did not make simulation with that. It is clear, that only very small differences occurred in the canopy layers. Values by M scenario are smaller than by G in each layer, both for temperature and vapor pressure. The largest differences were in the bottom layer for the temperature and vapor pressure, but they did not exceed 0.15 °C and 0.4 hPa, respectively. For wind speed, actually, there is no difference between the two scenarios.

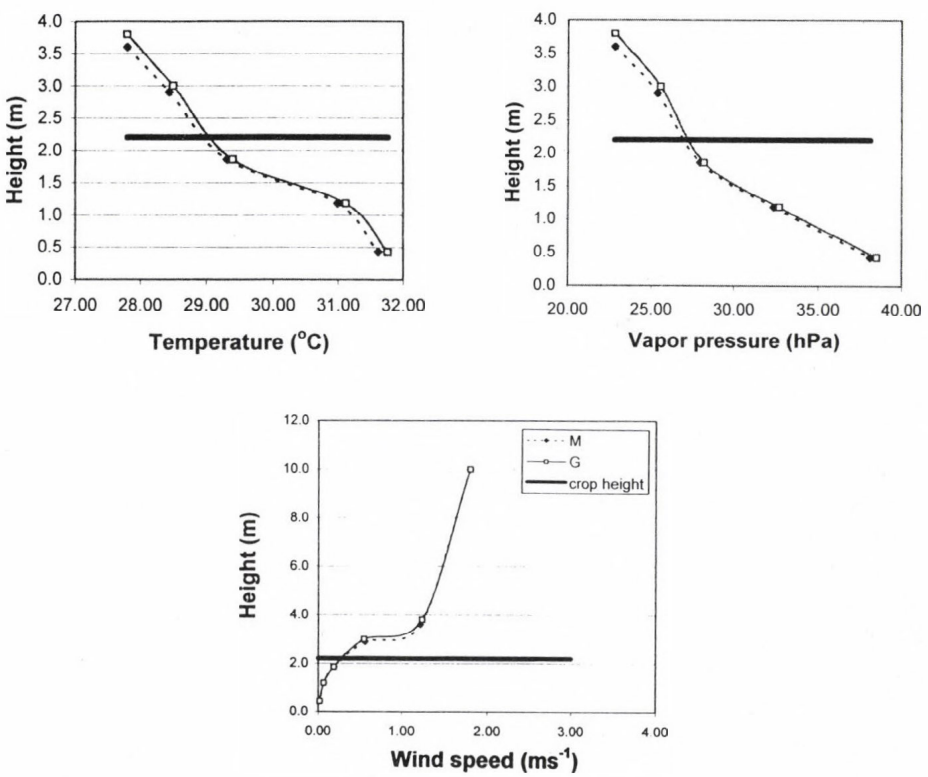

Fig. 5. Profiles of meteorological elements inside and above the canopy calculated by CMSM (on July 20,1999, 12:00 CET) using different height for the reference level; M: h_r=3.6 m, G: h_r=3.8 m. Signs are positioned at the middle of the layers.

5. Conclusions

Micrometeorological simulation models are useful tools to get information about the environmental conditions for photosynthesis, transpiration, and evaluation of mass and energy exhange between the vegetated surface and the atmosphere. Application of this type of model is restricted because of their input data requirements, namely input meteorological data must be representative for a reference height above the canopy. Direct measurements of this kind of data are rare and expensive. At the same time, automation of standard meteorological measurements is quite common, and those equipments provide meteorological data with high frequency in time. Data assimilation can be solved by data transformation. In that process some plant characteristics have to be taken into account. This study showed that at least plant height must be determined to get the surface roughness parameters. Further plant characteristics make the transferring process more sophisticated, but the actual values of modeled profiles inside the canopy are not influenced too much in the case of a normal maize stand. Nevertheless, when the vegetation is characterized by the same plant height, but *LAI* and drag properties of the leaves are different in great extent, the method of Goudriaan is suggested to determine surface roughness length and zero-plane displacement.

Further possibilities in application of micrometeorological models arise, when data from the nowcasting will be available for this purpose. Parametrization of the surface is extremely important in the nowcasting methods.

Acknowledgement—The study was supported by the Hungarian Scientific Research Fund (OTKA), the project number is T43147.

References

Ács, F., 1994: A coupled soil-vegetation scheme: description, parameters, validation, and sensitivity studies. *J. Appl. Meteorol. 33*, 268–284.

Ács, F. and *Hantel, M.*, 1998: Land-surface hydrology parametrization in PROGSURF: Formulation and test via Cabauw data. *Időjárás 102*, 109-127.

Ács, F. and *Hantel, M.*, 1999: The Penman-Monteith concept based land-surface model PMSURF. *Időjárás 103*, 19-36.

Ács, F. and *Kovács, M.*, 2001: The surface aerodynamic transfer parametrization method SAPA: description and performance analysis. *Időjárás 105*, 165-182.

Anda, A., Lőke, Zs., and *Varga, B.*, 2003: Possibility for using standard meteorological data as input for micrometeorological model (in Hungarian). *Légkör XLVIII 2*, 28-33.

Boegh, E., Soegaard, H., Friborg, T., and *Levy, P.E.*, 1999: Models of CO_2 and water vapor fluxes from a sparse millet crop in the Sahel. *Agr. Forest Meteorol. 93*, 7–26.

Chen, J., 1984a: Mathematical analysis and simulation of crop micrometeorology. *PhD Thesis*. Pudoc, Wageningen.

Chen, J., 1984b: Uncoupled multi-layer model for the transfer of sensible and latent heat flux densities from vegetation. *Bound.-Lay. Meteorol. 28*, 213-225.

Flerchinger, G.N., *Kustas, W.P.*, and *Weltz, M.A.*, 1998: Simulating surface energy fluxes and radiometric surface temperatures for two arid vegetation communities using the SHAW model. *J. Appl. Meteorol. 37*, 449–460.

Goudriaan, J., 1977: *Crop Micrometeorology: A Simulation Study*. Pudoc, Wageningen.

Hunkár, M., 1990: Simulation of microclimate of maize (in Hungarian). *Időjárás 94*, 221-229.

Hunkár, M., 2002: Moisture supply and microclimate- interactions with productivity potential. *Phys. and Chem of the Earth 27*, 1113-1117.

Hurtalova, T. and *Matejka, F.*, 1999: Surface characteristics and energy fluxes above different plant canopies. *Agric. Forest Meteorol. 98-99*, 491-500.

Hurtalova, T., *Matejka, F.*, *Chalupnikova, B.*, and *Rožnovský, J.*, 2004: Aerodynamic properties of air layer above maize canopy during windy conditions. *Időjárás 108*, 65-75.

Long, I.F., *Monteith, J.L.*, *Pennman, H.L.*, and *Szeicz, G.*, 1964: The plant and its environment. *Meteorol. Rundsch. 17*, 97-101.

Monteith, J.L., 1973: *Principles of Environmental Physics*. Edward Arnold, London.

Munroe, D.S. and *Oke, T.R.*, 1973: Estimating wind profile parameters for tall dense crops. *Agr. Meteorol. 11*, 223-228.

Sellers, P.J., *Randall, D.A.*, *Collatz, G.J.*, *Berry, T.A.*, and *Field, C.B.*, 1996. A revised land surface parameterization (SIB2) for atmospheric GCMs. Part I: Model formulation. *J. Climate 9*, 676–705.

Shaw, R.H., *den Hartog, G.*, *King, K.M.*, and *Thurtell, G.W.*, 1974: Measurements of mean wind flow and three dimensional turbulence within mature corn canopy. *Agr. Meteorol. 13*, 419-425.

Stanhill, G., 1969: A simple instrument for the field measurement of turbulent diffusion flux. *J. Appl. Meteorol. 8*, 509-513.

Szász, G. and *Tőkei, L.* (eds.), 1997: *Meteorology for Agronomist, Gardeners and Foresters* (in Hungarian). Mezőgazda, Budapest.

Tajchman, S.J., 1981: Comments on measuring turbulent exchange within and above forest canopy. *B. Am. Meteorol. Soc. 62*, 1550-1559.

Tanner, C.B. and *Pelton, W.L.*, 1960: Potential evapotranspiration estimates by approximate energy balance method of Penman. *J. Geophys. Res. 65*, 3391-3413.

Tourula, T. and *Heikiheimo, M.*, 1998: Modeling evapotranspiration from a barley field over the growing season. *Agr. Forest Meteorol. 91*, 237–250.

Weidinger, T., *Pinto, J.*, and *Horváth, L.*, 2000: Effects of uncertainities in universal functions, roughness length, and displacement height on the calculation of surface layer fluxes. *Meteorol. Z. 9*, 139-154.

Wieringa, J., 1993: Representaive roughness parameters for homogeneous terrain. *Bound.-Lay. Meteorol. 63*, 323-363.

IDŐJÁRÁS

Quarterly Journal of the Hungarian Meteorological Service
Vol. 109, No. 1, January–March 2005, pp. 55–67

On some climatic changes in the circulation over the Mediterranean area

Tania Marinova, Lilia Bocheva and **Vladimir Sharov**

National Institute of Meteorology and Hydrology,
66 Tsarigradsko Chaussee, Sofia 1784, Bulgaria
E-mails: Tania.Marinova@meteo.bg; Lilia.Bocheva@meteo.bg

(Manuscript received in final form January 14, 2005)

Abstract–Global climate changes affect the atmospheric circulation over the European synoptic region and, in particular, over the Mediterranean. In recent years the activity of cyclogenesis has strongly diminished over the Western Mediterranean and is not typical for the eastern part of the region. The present work is a climatological investigation of synoptic scale Mediterranean cyclones in relation to the number of cyclones originating over the Mediterranean, their paths of movement, and the interannual activity of the Mediterranean center. A study was carried out using surface pressure charts from the Synoptic Archive of the National Institute of Meteorology and Hydrology of Bulgaria for the period 1980–2001. The comparison of the derived results with the results of other authors obtained for previous periods show a well pronounced decrease in the number of Mediterranean cyclones. At the same time, the activity of the Mediterranean center during the course of a year is about two months shorter. After 1990, considerable changes in the regular paths of Mediterranean cyclones were observed.

Key-words: Mediterranean cyclones, cyclonic activity and frequency, paths of movement

1. Introduction

The Mediterranean basin is well known as a favored region for cyclone formation, especially during the cold half of the year, when depressions are more pronounced and deeper, with magnitude of their central pressure often below 1005 hPa. The winter cyclonic activity over the area is related to the appropriate thermal conditions. These conditions are provided by the specific orography – a warm sea surface, surrounding by mountain massifs that stop

cold air advection from Western and Central Europe. At the same time, the tropical Atlantic and African air masses enter the Mediterranean unimpeded. Therefore, an active frontal zone, with large baric and temperature gradients, having seasonal quasi-stationary front characteristics, forms over the Mediterranean.

The Mediterranean cyclones and their formation, frequency, trajectories, and influence on weather and climate over the region, are presented by many authors such as *Martinov* (1967), *Blagoev* (1961), *Stanchev* (1954), *Pisarski* (1955a,b), *Radinovic* (1987), *Reiter* (1975). In their studies, the cyclones are identified and classified on the basis of synoptic charts for specific areas of the Mediterranean region.

Recently *Alpert et al.* (1990), *Trigo et al.* (1999), and *Maheras et al.* (2001) have presented cyclone climatologies based on objective methods for periods of 5, 18, and 40 years, respectively. These studies revealed three major centers of maximum cyclonic frequency: the Gulf of Genoa, Southern Italy, and Cyprus. The cyclones are identified with the aid of an objective method based on grid point values, available every 6 hours, and include all the initial cyclone detections, that is, cyclones developing within the Mediterranean basin plus cyclones entering the domain. *Alpert et al.* (1990) in his work focused on the month to month variations in cyclone tracks over the Mediterranean. *Trigo et al.* (1999) performed objective cyclone detection and tracking analysis in the Mediterranean region using a higher resolution dataset over a period of 18 years. A greater number of trajectories, including those for subsynoptic lows, were analyzed. The results were summarized by submitting the monthly trajectories (for January, April, and August only) to a k-means clustering procedure.

This paper presents a climatological investigation of subjectively selected synoptic scale Mediterranean cyclones using synoptic charts over a 22-year period from 1980 to 2001. A study was carried out comparing the derived results with the results of other authors obtained for previous periods of time. A series of differences were found in relation to the number of the cyclones originating in the Mediterranean, the interannual activity of the Mediterranean center, and the paths of movement of Mediterranean cyclones.

2. Cyclonic activity over the Mediterranean

The present study concerns the region between 30–45°N and 5°W–30°E. Only newly originating cyclones, which had at least one closed isobaric line on the synoptic surface chart (standard analysis with 5 hPa isobars) and a duration of more than 30 hours were considered. On the basis of surface pressure charts

from the Synoptic Archive of the National Institute of Meteorology and Hydrology of Bulgaria, the surface centers of the cyclones originating over the concerned area were plotted on special charts, from the time of the first closed isobar appearance. Furthermore, for every case, the location of the surface center over the area was plotted at 00 UTC. The time of the chart, where closed isobaric lines were observed for the last time, was accepted as the end of the process. All events were plotted on charts for the different years of the period. For the period 1990–1999, the locations of origination and trajectories of the cyclones were plotted for different months of the year, in order to study possible changes of cyclogenetic areas, as well as the paths of movement of the Mediterranean cyclones during the course of the year.

The summarized results for the monthly and annual distribution of cyclones originating over the Mediterranean area during the period 1980–2001 are presented in *Table 1*. It can be seen that cyclone frequency is the strongest in winter from December until March. On average, over the 22 years of consideration, there are cyclones every 16 to 17 days. The cyclonic activity decreases in April, when originated cyclones occur 3 times less frequently than in March. From May to September, cyclogenesis is a rare phenomenon in the region. The number of originated cyclones strongly increases in November – 4 times more than the previous month, while in October there are 30% more than in September. In November, the cyclogenesis over the region reaches its characteristic frequency for the cold part of the year, i.e., in autumn well pronounced transition to the Mediterranean center activation is not observed.

In comparison with similar climatic investigations by different authors for earlier periods – *Martinov* (1967), *Blagoev* (1961), *Stanchev* (1954), *Pisarski* (1955a,b), *Radinovic* (1987), *Reiter* (1975) – our results indicate that the duration of the Mediterranean winter cyclonic center activity within a year is shorter. All the above authors have given October as the beginning of the Mediterranean winter cyclone, while presented results indicate strong activation of cyclogenesis in November. Also, they have concluded that May is the transition month when the seasonal center is reduced, in contrast to our results which show April. During the period of study, there is a two-month decrease in the activity of the Mediterranean winter cyclones. In all studies, the seasonal character of the Mediterranean center activation is mentioned. Cyclogenesis during the cold half of the year (from October to March) occurs 3 times more often than during the warm half of the year (*Pisarski*, 1955b), while in our study it is more than 5 times larger for the entire investigated period.

Most of the authors dealing with climatic characteristics of the Mediterranean area, cyclogenesis conditions, frequency of originating and principal paths of depressions, as well as their influence on some climatic

Table 1. Annual and monthly distribution of the cyclones originating over the Mediterranean area for the period 1980–2001

Year→ Month	Number of cyclones																								
	´80	**´81**	**´82**	**´83**	**´84**	**´85**	**´86**	**´87**	**´88**	**´89**	**´90**	**´91**	**´92**	**´93**	**´94**	**´95**	**´96**	**´97**	**´98**	**´99**	**´00**	**´01**	**Sum 1980-1989**	**Sum 1990-1999**	**Sum 1980-2001**
Jan	5	4	2		2	1	5	1	3	1					4	3	1	1	1	3	1	3	24	13	41
Feb	2	3	2	2	1	2	3	3	2		1	1	1	2	4		3	1	1	1	1	1	20	15	37
Mar	3	2	7	4	2	2	2	5	3	3			2	1		2			2		1		33	7	41
Apr	3					1		1			1		1	1	1		1	1			2	2	5	6	15
May	2	1	1	1								2											5	2	7
Jun		1	1									1											2	1	3
Jul		1		1																			2	0	2
Aug	1			1					1	1													4	0	4
Sep		1			1				1	1						1	1						4	2	6
Oct	1	2		2						1		1						2					6	3	9
Nov	1	2	2	1			1	3	3	2	3	1	1	1	2	3	1	2	2	1			15	17	32
Dec	4	5	1	3		1	2		2	2	3	2	1	1	1	3	2	2	1	2	1	1	20	18	41
General number	**22**	**22**	**16**	**15**	**6**	**7**	**14**	**13**	**15**	**11**	**8**	**8**	**6**	**6**	**12**	**12**	**9**	**9**	**7**	**7**	**6**	**7**	**141**	**84**	**238**

elements in the adjacent regions and in particular in Bulgaria, work with data for a 9–10 years period. For better comparison of our results with the results of other authors, two 10-year periods were determined: the first from 1980 to 1989, the second from 1990 to 1999. However, it is not possible to use the same investigation methods, as the different authors. Each method is based on a different approach for selecting a region, duration, and type of depressions to study. Most similar to this investigation are the studies of *Blagoev* (1961), *Radinovic* (1987), and to a certain degree *Martinov* (1967, 1983). The last one takes into consideration only well pronounced baric formations which originate or pass over the Balkan Peninsula; information about the duration of each of the processes is not given. In *Table 2* the number of Mediterranean cyclones is presented for the periods 1980–1989 and 1990–1999, in addition to other periods according to *Blagoev* (1961), *Radinovic* (1987), and *Martinov* (1967).

Table 2. Number of Mediterranean cyclones for different periods

Author	Period	Total number of cyclones	Average annual number of cyclones
Blagoev (1961)	1951–1960	295	29
Radinovic (1987)	1951–1960	283	28
Martinov (1967)	1958–1966	165	18
Our team	a. 1980–1989	148	15
	b. 1990–1999	84	8

If one examines the two 10-year periods (*Table 1*) separately, it can be seen that during the period 1980–1989, the cyclogenesis becomes weaker, although, it follows the interannual distribution described in earlier studies of other authors. In the period 1990–1999, a well pronounced decrease in the number of originated cyclones is observed in comparison with the results of the authors given in *Table 2*. In addition, the part of the year with the greatest activity of the Mediterranean center is shorter. For the first period the cyclogenesis over the Mediterranean in the cold half of the year is about 5 times greater than that during the rest of the year. For the second period it is about 7 times greater.

Further presented results concern only the period 1990–1999. During this period, the greatest activity of the Mediterranean center is observed in November, December, January, and February. In March the number of cyclones that originate over the Mediterranean is 2 times less than in February, and almost equals to that in April. In comparison, *Martinov* (1967) and *Pisarski* (1955b) conclude that in March cyclogenesis is more active than in

February. They also describe the almost equal number of originated cyclones in February and April, which only in May decreases approximately 2 times compared to April. During the period 1990–1999, only 7 cyclones originated in March and again, like typical winter months, their cyclogenetic area is in the region of the Gulf of Genoa, the Iberian Peninsula, and the Adriatic Sea. In April, there were 6 cases of cyclones originating mainly in the region of Ligurian and Tyrrhenian Sea around the Islands of Sardinia and Corsica.

It can be summarized that during the period 1990–1999, cyclogenesis over the Mediterranean was located mainly in its central parts, in the area of the Gulf of Genoa, the Ligurian and the Tyrrhenian Sea, the Iberian Peninsula, and in rarer cases, over the Adriatic and Ionian Sea. In view of the changed circulation conditions over the area in January and February, even in the case of the southernmost position of the seasonal quasi-stationary front and the line of negative heat balance, the meridional circulation is predominant. Consequently, the orographic cyclogenesis over the Alps continues to be the dominant cyclogenetic factor in the area. Nevertheless, there are some isolated cases of cyclones originating over the Gulf of Lion and to the east of the Balearic Islands. In January and February intensive cyclonic activity is observed over the southern parts of the Atlantic Ocean. As a result of the more northern position of the active frontal zone, the series of Atlantic cyclones pass to the east through the northern part of the Iberian Peninsula and France (i.e., they propagate and fill in Central Europe). The movement of the frontal zone from its usual position to the north by about 300 km (2–3°) in the spring months leads to a decreasing number of cyclones originating in March and April.

3. Paths of movement of Mediterranean cyclones in the period 1990–1999

The first studies on the trajectories of Mediterranean cyclones were carried out more than hundred years ago in order to explain the weather conditions in different regions of Europe. *Van Bebber* (1891) presented a scheme in which the main path of the South European cyclones were indicated by the Roman letter V, and the variants of this path were indicated by the Arabic letters Vb, Vc, Vd, Vd_1, Vd_2.

Later, the principal paths of Mediterranean cyclones and their seasonal peculiarities were studied by many authors: *Pisarski* (1955a), *Blagoev* (1961), *Martinov* (1983), *Popova et al.* (1975). More recently, the tracks of surface depressions coming into and passing trough the Mediterranean were described objectively by *Alpert et al.* (1990) and *Trigo et al.* (1999), but they only detected trajectories in the corresponding observed region. In almost all of the studies until now, 3 principal paths of movement are mentioned: I. To the

northeast through Croatia and Hungary; II. To the east through the Adriatic Sea and the Balkan Peninsula towards the Black Sea; III. To the east–southeast through the southernmost parts of the Balkan Peninsula towards Asia Minor. A generalized scheme of the principal cyclogenetic areas and of the paths of cyclone movement from west to east or from southwest to northeast is given in *Fig. 1*.

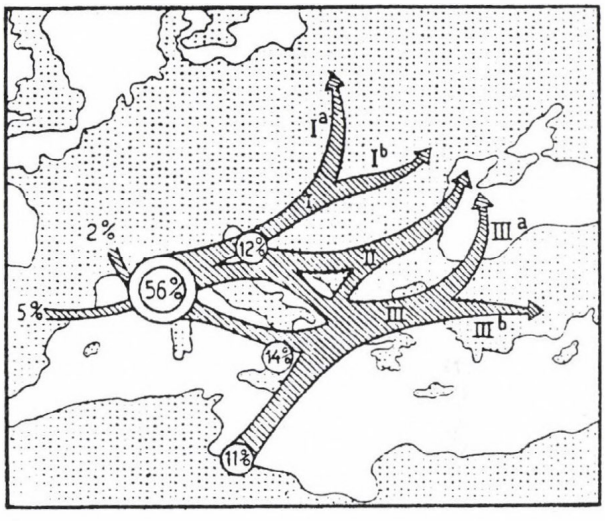

Fig. 1. Areas of generation and paths of movement of Mediterranean cyclones (after *Pisarski*, 1955a).

The derived results indicate considerable changes in the regular paths of cyclones after the year 1980, especially during the period 1990–1999.

The surface centers of cyclone origin were plotted on special charts for each month of the year, and in every case the cyclone paths were followed for the period 1990–1999.

The results of *Martinov* (1983) are used for comparison, as his work followed a similar approach to determine peculiarities in the paths of movement of Mediterranean cyclones in the different months. For each month, from November to April, the main paths of Mediterranean cyclones were plotted on the same chart after *Martinov* (1983) (solid curves) for the period 1958–1966, as well as our results for the period 1990–1999 (dashed curves).

According to *Martinov* (1983), in November (*Fig. 2*) activation of cyclogenesis is observed in the area of the Gulf of Genoa and Southern Italy, but only a small number of the cyclones move towards the Balkan Peninsula

and Bulgaria. The cyclones originating in the western parts of the Mediterranean basin are stationary or move eastward to Central Italy and the Adriatic Sea, where they fill. The rest of the cyclones move along the northwestern path to Hungary or eastward across the southernmost regions of the Balkan Peninsula, and from there northeastward to Crimea. In the period 1990–1999, a large part of the cyclones move across the Balkan Peninsula. From the Gulf of Genoa, part of the cyclones move through Northern Italy and the northern part of the Adriatic Sea, further northeastward to Romania and from there, southeastward to the Black Sea, where they fill.

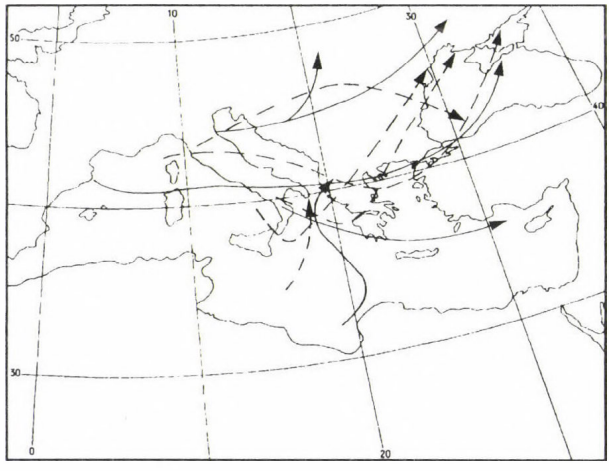

Fig. 2. Paths of movement of Mediterranean cyclones in November for the periods 1958–1966 (solid curves) and 1990–1999 (dashed curves).

Another part of the cyclones originating in the West Mediterranean follow a more southern path through the Apennines, the South Adriatic, and southern parts of the Balkan Peninsula towards Asia Minor and Crimea. A very small portion of the cyclones originating around the Islands of Sardinia, Corsica, and over the Central Mediterranean move through Southern Italy and the Ionian Sea, where they fill. In general, it can be said that about 2/3 of the studied cyclones in November continue their path over the Balkan Peninsula. However, a very small portion of them move across Bulgaria, as most of these cyclones pass south and southeast of the country.

The tendency of cyclones to move mainly along their southernmost paths and eastward across the Balkan Peninsula is retained in December (*Fig. 3*). The characteristic movement of cyclones originating in the West

Mediterranean along the northwestern path through Croatia and Hungary as described by *Martinov* (1983) is not observed. In the present study, a part of the cyclones originating around the Gulf of Genoa and the Island of Corsica move eastward across the North Adriatic and the Balkan Peninsula (and Bulgaria) towards the Black Sea. Another part from Northern Italy and the region of the Tyrrhenian Sea move southeastward over the Ionian Sea, Central Greece, then towards Asia Minor, and from there through the eastern parts of the Black Sea.

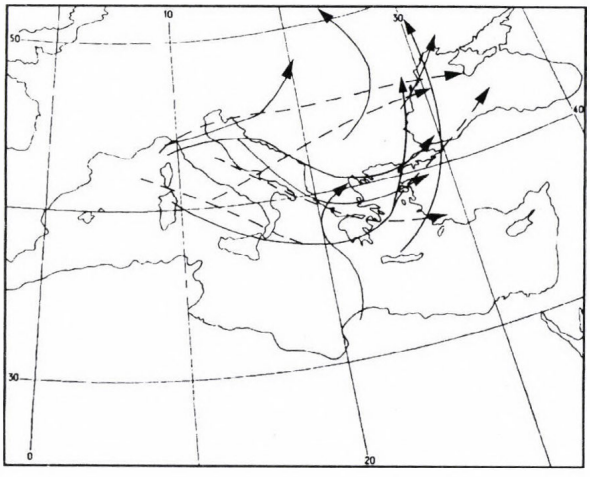

Fig. 3. Paths of movement of Mediterranean cyclones in December for the periods 1958–1966 (solid curves) and 1990–1999 (dashed curves).

Cyclones in January (*Fig. 4*) have the best outline paths resembling those described by *Martinov* (1983). A well defined zone of cyclone movement emerges clearly. The cyclones move from the Northwest Mediterranean and the central parts of the Apennines southeast across Italy, the Ionian Sea, the Island of Crete, and then northeast towards Asia Minor. This principal path of movement of Mediterranean cyclones is joined by additionally generated cyclones over the Ionian Sea.

In February (*Fig. 5*) some changes occur in the paths of Mediterranean cyclones. A significant part of cyclones originate over the central part of the Mediterranean Sea (along the northern coasts of Africa), but not over the Gulf of Genoa and Balearic Islands as in *Martinov* (1983). Initially they move northeastward to Southern Italy, where a small part of them fill. The largest

part, together with the cyclones originating over the Tyrrhenian Sea, move eastward across the Ionian Sea, Southern Greece, and the Island of Cyprus. From there they move eastward or northeastward across the Black Sea to Crimea. Very few cyclones move from the Gulf of Genoa and the Adriatic Sea straight eastward across the Balkan Peninsula and Bulgaria.

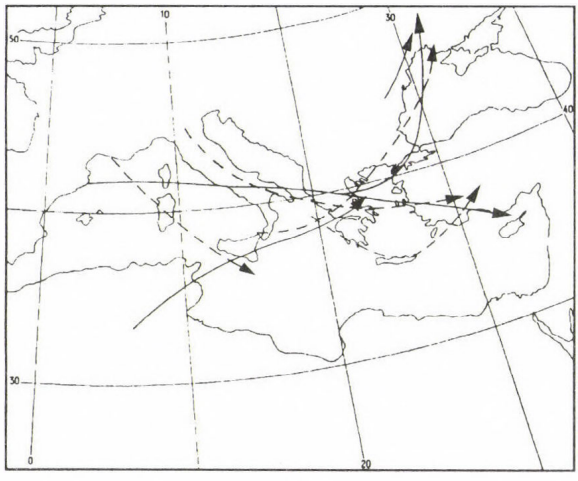

Fig. 4. Paths of movement of Mediterranean cyclones in January for the periods 1958–1966 (solid curves) and 1990–1999 (dashed curves).

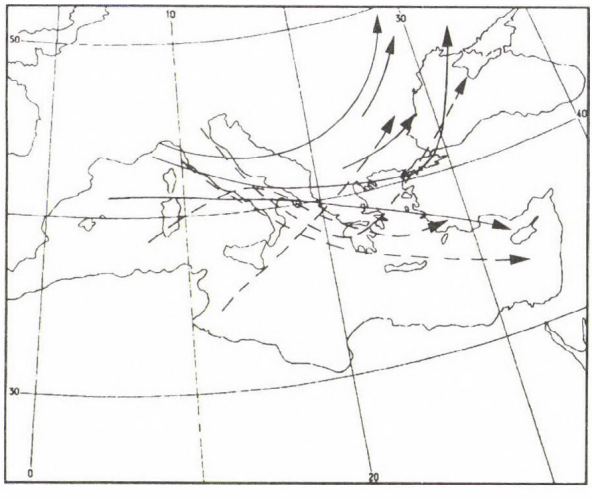

Fig. 5. Paths of movement of Mediterranean cyclones in February for the periods 1958–1966 (solid curves) and 1990–1999 (dashed curves).

In March (*Fig. 6*) there is a decrease in the number of cyclones generated over the Mediterranean and a shift of the cyclogenetic regions to the east over the Apennines, the Adriatic, and the Ionian Sea. All generated cyclones move to the east – northeast either across or south of the Balkans. There are no cyclones passing in a northwestern direction across Croatia and Hungary, and this cyclogenesis is not typical in the West Mediterranean. A portion of the cyclones passing across the southernmost regions of Greece move towards the Island of Cyprus, and others move eastward across Asia Minor. From there they move northeastward across the Black Sea towards Crimea. The trajectory of the cyclones originating along the northern coasts of Africa is orientated to the northeast across the Balkan Peninsula towards Ukraine.

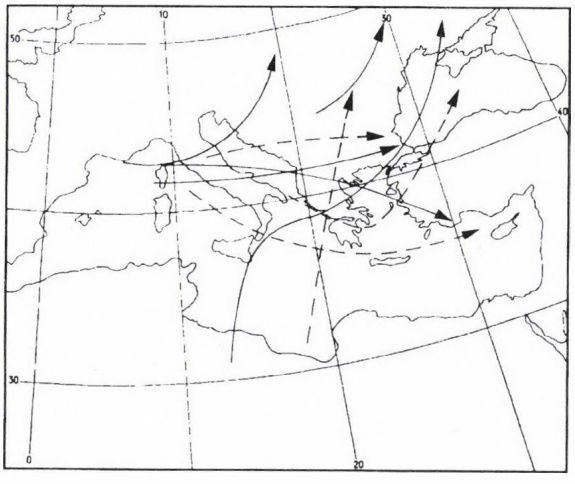

Fig. 6. Paths of movement of Mediterranean cyclones in March for the periods 1958–1966 (solid curves) and 1990–1999 (dashed curves).

Cyclogenesis in April (*Fig. 7*) is very weak and located over the West Mediterranean, in the region of the Balearic Islands, the Island of Sardinia, and the African coast. The trajectories of these cyclones cannot be arranged in groups. A portion of the cyclones moves southeastward and fill in the region of Southern Italy. Others move eastward across the southernmost areas of the Balkan Peninsula towards Asia Minor, where they join cyclones originating near North Africa. Again, there are no cyclones moving along the northwestern path across Croatia and Hungary.

Considering the paths of cyclones originated over the Mediterranean in the period 1990–1999, it can be concluded, that the greatest number of

depressions pass across the southernmost part of the Balkan Peninsula. Their influence on the weather in Turkey and Greece is the most significant. Bulgaria remains mostly in the northern periphery of the cyclonic vortex, and therefore, the meteorological phenomena connected with cyclones are decreased. More considerable changes in temperature, pressure, and especially in precipitation are observed, when the cyclonic vortex moves directly across the Balkans and northeastward across the Black Sea.

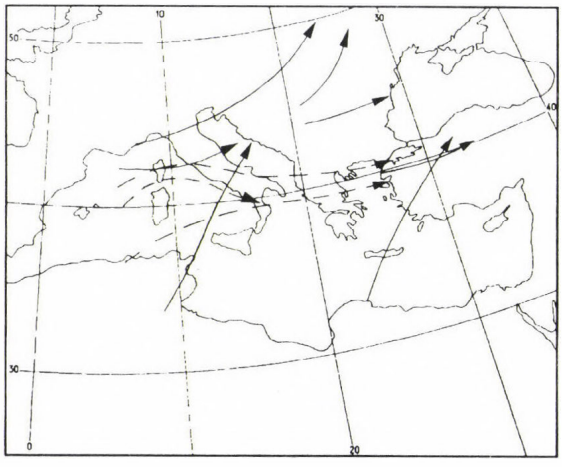

Fig. 7. Paths of movement of Mediterranean cyclones in April for the periods 1958–1966 (solid curves) and 1990–1999 (dashed curves).

4. Conclusions

The results obtained in the present work can be summarized as follows:

- A well pronounced decrease in the number of Mediterranean cyclones is observed during the period 1980–2001. At the same time, the activity of the Mediterranean winter cyclonic center within a year is about two months shorter.
- After 1990, cyclogenesis over the Mediterranean is located mainly in its central parts. Considerable changes of the regular paths of cyclones are observed. The greatest number of Mediterranean cyclones pass across the southernmost part of the Balkan Peninsula. The principal path of movement, to the northeast through Croatia and Hungary, is no longer typical for the Mediterranean cyclones nowadays.

References

Alpert, P., Neeman, B.U., and *Shay-El, Y.,* 1990: Intermonthly variability of cyclone tracks in Mediterranean. *J. Climate 3*, 1474-1478.

Blagoev, Ch., 1961: Routes of the Mediterranean Sea cyclones (in Bulgarian). *Hydrol. Meteorol. 1*, 43-51.

Maheras, P., Flocas, H.A., Patricas, I., and *Anagnostopoulou, Chr.*, 2001: A 40-year objective climatology of surface cyclones in the Mediterranean region: Spatial and temporal distribution. *Int. J. Climatol. 21*, 109–130.

Martinov, M., 1967: Some peculiarities of cyclogenesis in the region of the Mediterranean Sea and the Balkan Peninsula (in Bulgarian). *Hydrol. Meteorol. 6*, 7–21.

Martinov, M., 1983: Synoptical and statistical processing of historical data for Mediterranean depressions. *PSMP Report Series*. Short- and medium-range weather prediction research publication series, No. 3, 121–144.

Pisarski, A., 1955a: The Mediterranean cyclones and their influence on the weather in Bulgaria. Part I (in Bulgarian). *Hydrol. Meteorol. 5*, 33-50.

Pisarski, A., 1955b: The Mediterranean cyclones and their influence on the weather in Bulgaria. Part II (in Bulgarian). *Hydrol. Meteorol.6*, 3–15.

Popova, T., Runcanu, T. Tanczer, T., and *Sharov, V.*, 1975: *Mediterranean Cyclones in the Cloud Field* (in Russian). Gidrometeoizdat, Leningrad, 98p.

Radinovic, D., 1987: Mediterranean cyclones and their influence on the weather and climate. *PSMP Report Series,* No. 24, 131.

Reiter, E., 1975: Handbook for Forecasters in the Mediterranean, Environmental Prediction Research Facility. Naval Postgraduate School, Monterey, Californy. *Tech. Paper,* No. 5–75, 344.

Stanchev, K., 1954: The South cyclones, their moving through the Balkan Peninsula and the weather in Bulgaria determined by them (in Bulgarian). *Hydrol. Meteorol. 5*, 19–39.

Trigo, I.F., Davies, T.D., and *Bigg, G.R.,* 1999: Objective climatology of cyclones in the Mediterranean region. *J. Climate 12*, 1685–1696.

Van Bebber, W.J., 1891: Die Zugstrassen der barometrischen Minima nach den Bahnenkarten Deutschen Seewarte für den Zeitraum von 1875–1890. *Meteorol. Z. 8*, 361–366.

BOOK REVIEW

J. M. Pap and *P. Fox* (eds.): **Solar Variability and Its Effects on Climate.** Geophysical Monographs 141, American Geophysical Union, 2004, Washington D.C., 366 pages.

This book is a collection of papers dealing with our variable star (the Sun), and the terrestrial atmospheric and climate variations related to the solar changes. The editorial work had been helped by five contributing editors. The total number of papers is 24. The questions that are answered (on the basis of the most recent surface and satellite measurements) are the following:

- What physical processes occur in the various parts of the solar interior and atmosphere and how these processes relate to variations in solar energy flux at time scales ranging from solar evolution to decades and minutes?

- How do changes in the solar energy flux and energetic particle flux influence Earth's atmosphere and this way its climate?

The papers are divided into four sections. The first section (Fundamentals, 6 items) treats the up-to-date knowledge of solar physics and a short overview of the Earth's atmosphere and climate. The next section (Solar Energy Flux Variations, 8 items) describes the variations of total and spectral irradiation of the Sun as well the variations of solar output of energetic particles. Section 3 (Solar Variability and Climate, 9 items) shows the relations between the above mentioned variations and the changes of the climate of our planet. The last section (1 item) looks at the future, basically at the science requirements and the necessary measurements.

The well-written articles in the logically structured book are proposed to those scientists who are interested in understanding and predicting solar changes and their influences on our climate.

G. Major

GUIDE FOR AUTHORS OF *IDŐJÁRÁS*

The purpose of the journal is to publish papers in any field of meteorology and atmosphere related scientific areas. These may be

- research papers on new results of scientific investigations,
- critical review articles summarizing the current state of art of a certain topic,
- short contributions dealing with a particular question.

Some issues contain "News" and "Book review", therefore, such contributions are also welcome. The papers must be in American English and should be checked by a native speaker if necessary.

Authors are requested to send their manuscripts to

Editor-in Chief of IDŐJÁRÁS
P.O. Box 39, H-1675 Budapest, Hungary

in three identical printed copies including all illustrations. Papers will then be reviewed normally by two independent referees, who remain unidentified for the author(s). The Editor-in-Chief will inform the author(s) whether or not the paper is acceptable for publication, and what modifications, if any, are necessary.

Please, follow the order given below when typing manuscripts.

Title part: should consist of the title, the name(s) of the author(s), their affiliation(s) including full postal and E-mail address(es). In case of more than one author, the corresponding author must be identified.

Abstract: should contain the purpose, the applied data and methods as well as the basic conclusion(s) of the paper.

Key-words: must be included (from 5 to 10) to help to classify the topic.

Text: has to be typed in double spacing with wide margins on one side of an A4 size white paper. Use of S.I. units are expected, and the use of negative exponent is preferred to fractional sign. Mathematical formulae are expected to be as simple as possible and numbered in parentheses at the right margin.

All publications cited in the text should be presented in a *list of references*, arranged in alphabetical order. For an article: name(s) of author(s) in Italics, year, title of article, name of journal, volume, number (the latter two in Italics) and pages. E.g., *Nathan, K.K.,* 1986: A note on the relationship between photo-synthetically active radiation and cloud amount. *Időjárás 90,* 10-13. For a book: name(s) of author(s), year, title of the book (all in Italics except the year), publisher and place of publication. E.g., *Junge, C. E.,* 1963: *Air Chemistry and Radioactivity*. Academic Press, New York and London. Reference in the text should contain the name(s) of the author(s) in Italics and year of publication. E.g., in the case of one author: *Miller* (1989); in the case of two authors: *Gamov* and *Cleveland* (1973); and if there are more than two authors: *Smith et al.* (1990). If the name of the author cannot be fitted into the text: *(Miller,* 1989); etc. When referring papers published in the same year by the same author, letters a, b, c, etc. should follow the year of publication.

Tables should be marked by Arabic numbers and printed in separate sheets with their numbers and legends given below them. Avoid too lengthy or complicated tables, or tables duplicating results given in other form in the manuscript (e.g., graphs)

Figures should also be marked with Arabic numbers and printed in black and white in camera-ready form in separate sheets with their numbers and captions given below them. Good quality laser printings are preferred.

The text should be submitted both in manuscript and in electronic form, the latter on diskette or in E-mail. Use standard 3.5" MS-DOS formatted diskette or CD for this purpose. MS Word format is preferred.

Reprints: authors receive 30 reprints free of charge. Additional reprints may be ordered at the authors' expense when sending back the proofs to the Editorial Office.

More information for authors is available: antal.e@met.hu

Information on the last issues: http://omsz.met.hu/irodalom/firat_ido/ido_hu.html

Published by the Hungarian Meteorological Service

Budapest, Hungary

INDEX: 26 361

HU ISSN 0324-6329